Molecular Biology of the Cell
Vol. 16, 4108–4123, September 2005

The *Salmonella* Effector PipB2 Affects Late Endosome/Lysosome Distribution to Mediate Sif Extension[V]

Leigh A. Knodler and Olivia Steele-Mortimer

Laboratory of Intracellular Parasites, Rocky Mountain Laboratories, National Institutes of Allergy and Infectious Diseases, National Institutes of Health, Hamilton, MT 59840

Submitted April 29, 2005; Revised June 16, 2005; Accepted June 17, 2005
Monitoring Editor: Ralph Isberg

After internalization into mammalian cells, the bacterial pathogen *Salmonella enterica* resides within a membrane-bound compartment, the *Salmonella*-containing vacuole (SCV). During its maturation process, the SCV interacts extensively with host cell endocytic compartments, especially late endosomes/lysosomes (LE/Lys) at later stages. These interactions are mediated by the activities of multiple bacterial and host cell proteins. Here, we show that the *Salmonella* type III effector PipB2 reorganizes LE/Lys compartments in mammalian cells. This activity results in the centrifugal extension of lysosomal glycoprotein-rich membrane tubules, known as *Salmonella*-induced filaments, away from the SCV along microtubules. *Salmonella* overexpressing *pipB2* induce the peripheral accumulation of LE/Lys compartments, reducing the frequency of LE/Lys tubulation. Furthermore, ectopic expression of *pipB2* redistributes LE/Lys, but not other cellular organelles, to the cell periphery. In coexpression studies, PipB2 can overcome the effects of dominant-active Rab7 or Rab34 on LE/Lys positioning. Deletion of a C-terminal pentapeptide motif of PipB2, LFNEF, prevents its peripheral targeting and effect on organelle positioning. The PipB2 homologue PipB does not possess this motif or the same biological activity as PipB2. Therefore, it seems that a divergence in the biological functions of these two effectors can be accounted for by sequence divergence in their C termini.

INTRODUCTION

As part of their intracellular lifestyle, many pathogens survive and replicate within membrane-bound vacuoles that interact extensively with the host cell endocytic pathway. One classical example is the facultative intracellular bacterium *Salmonella enterica*. After internalization, *Salmonella* is enclosed within discrete vacuoles known as *Salmonella*-containing vacuoles (SCV). Initially, the SCV interacts transiently with early endosomes (Steele-Mortimer *et al*., 1999), but it rapidly matures, in a Rab7 GTPase- and phosphoinositide-dependent manner (Méresse *et al*., 1999; Scott *et al*., 2002; Hernandez *et al*., 2004) to bear a subset of late endosome/lysosome (LE/Lys) markers, including lysosomal-associated membrane protein (LAMP)-1, LAMP-2, cathepsin D, and lysobisphosphatidic acid (LBPA) (Garcia-del Portillo and Finlay, 1995; Brumell *et al*., 2001). The mature SCV is juxtanuclear, associates with the Golgi apparatus, and requires microtubules and microtubule motors for its positioning and homeostasis (Salcedo and Holden, 2003; Guignot *et al*., 2004; Harrison *et al*., 2004; Marsman *et al*., 2004; Boucrot *et al*., 2005).

After a lag-phase of 4–6 h in nonphagocytic cells and 9–12 h in phagocytic cells, bacterial replication is initiated and extensive membrane tubules, known as *Salmonella*-induced filaments (Sifs), extend from the SCV (Garcia-del Portillo *et al*., 1993; Freeman *et al*., 2003; Knodler *et al*., 2003). In uninfected cells, LE/Lys occupy a predominantly perinuclear location and a number of proteins contribute to their biogenesis, positioning and functioning including Rab7 (Bucci *et al*., 2000), Rabring7 (Mizuno *et al*., 2003), Rab-interacting lysosomal protein (RILP) (Cantalupo *et al*., 2001; Jordens *et al*., 2001), Rab34 (Wang and Hong, 2002), Vam6p/Vps39p (Caplan *et al*., 2001), Vps18p (Poupon *et al*., 2003) and microtubule motors (Burkhardt *et al*., 1997; Matsushita *et al*., 2004). Several of these mammalian proteins are also required for Sif formation (Brumell *et al*., 2001; Jordens *et al*., 2001; Guignot *et al*., 2004; Harrison *et al*., 2004). Sifs are lysosomal glycoprotein (lgp)-rich and represent the increased fusion of LE/Lys compartments along microtubules (Garcia-del Portillo *et al*., 1993; Brumell *et al*., 2002). Although Sifs are morphologically similar to tubular lysosomes observed in phagocytic cells (Hollenbeck and Swanson, 1990) they are distinct structures; Sifs are induced in nonphagocytic cells, where tubular lysosomes are not normally present, and require bacterial protein synthesis for their formation (Garcia-del Portillo *et al*., 1993). Mutants defective in Sif formation are attenuated for virulence (Hensel *et al*., 1998; Beuzon *et al*., 2000), implying that Sifs are important for the intracellular

This article was published online ahead of print in *MBC in Press* (http://www.molbiolcell.org/cgi/doi/10.1091/mbc.E05–04–0367) on June 29, 2005.

[V] The online version of this article contains supplemental material at *MBC Online* (http://www.molbiolcell.org).

Address correspondence to: Leigh A. Knodler (lknodler@niaid.nih.gov).

Abbreviations used: GFP, green fluorescent protein; HA, hemagglutinin; LAMP, lysosomal-associated membrane protein; LBPA, lysobisphosphatidic acid; LE/Lys, late endosomes/lysosomes; lgp, lysosomal glycoprotein; LPS, lipopolysaccharide; NDZ, nocodazole; PFA, paraformaldehyde; p.i., postinfection; RILP, Rab-interacting lysosomal protein; SCV, *Salmonella*-containing vacuole; Sif, *Salmonella*-induced filament; SPI, *Salmonella* pathogenicity island; TTSS, type III secretion system.

pathogenesis of *Salmonella*, although exactly how they contribute remains unknown.

Biogenesis and maintenance of the SCV and Sifs also depends upon *Salmonella* virulence factors, called effectors, that are translocated into the host cell by a type III secretion system (TTSS). *Salmonella* have two TTSS, encoded on *Salmonella* pathogenicity island-1 (SPI-1) and SPI-2, that function at distinct, but overlapping, phases of pathogenesis (reviewed in Hensel, 2004). The SPI-1 TTSS translocates effectors required for bacterial invasion of mammalian cells and some postinvasion events (reviewed in Knodler and Steele-Mortimer, 2003; Patel and Galan, 2005). In contrast, the SPI-2 TTSS is active inside host cells (Valdivia and Falkow, 1997; Cirillo *et al*., 1998) and translocates effectors across the SCV membrane. SPI-2 TTSS effectors contribute to numerous intracellular events, including vacuolar maturation, Sif formation, bacterial replication, and the systemic spread of bacteria (reviewed in Waterman and Holden, 2003; Kuhle and Hensel, 2004). At least eight effectors contribute to distinct aspects of SCV maturation and positioning, vacuole membrane integrity and Sif formation (Stein *et al*., 1996; Kuhle and Hensel, 2002; Ruiz-Albert *et al*., 2002; Salcedo and Holden, 2003; Jiang *et al*., 2004; Birmingham *et al*., 2005), but no mechanism of action has yet been defined for any of these. It has been difficult to attribute well-defined functions to individual effectors because many aspects of *Salmonella*'s interaction with host cells, including host cell invasion and vacuole maturation, require the cooperation of several type III effectors (Waterman and Holden, 2003; Kuhle and Hensel, 2004; Patel and Galan, 2005). As such, deletion of one effector often results in little to no phenotype in tissue cultured cells or animal models of infection.

The two SPI-2 TTSS effectors, PipB and PipB2, are homologues that share 29% identity and 55% similarity at the amino acid level (Knodler *et al*., 2003). Much of this sequence similarity is due to numerous tandem pentapeptide repeats, A(N/D)LXX, in their C-terminal domains. Such repeats are found in a variety of eukaryotic and prokaryotic proteins and are predicted to have a targeting or structural function (Bateman *et al*., 1998). Notably, the C termini of PipB and PipB2 are highly divergent. We have previously shown that translocated PipB and PipB2 have distinct intracellular localizations (Knodler *et al*., 2003). Both proteins localize to SCV and Sif membranes but PipB2 also is associated with vesicular-tubular structures at the cell periphery (Knodler *et al*., 2002, 2003). Furthermore, PipB and PipB2 seem to have distinct roles in pathogenesis. PipB is required for the cecal colonization of chicks (Morgan *et al*., 2004) and the induction of secretory and inflammatory responses in bovine ligated ileal loops (Wood *et al*., 1998), whereas PipB2 is required for virulence in a mouse model of infection (Knodler *et al*., 2003). The different localization patterns and contributions to virulence suggest a divergence of function for these two proteins.

Here, we show that, during a *Salmonella* infection, PipB2 activity is required for the radial extension of lgp-rich Sif tubules away from the juxtanuclear SCV. Ectopic expression of PipB2 in the absence of other bacterial proteins is sufficient to cause the redistribution of LE/Lys compartments, but not other organelles, to the cell periphery. Cotransfection of PipB2 with dominant-active Rab7 and Rab34 demonstrates that PipB2 acts downstream or in a parallel pathway to these proteins to regulate LE/Lys positioning. The type III effector homologue PipB does not affect LE/Lys positioning like PipB2. Sequence comparison of PipB and PipB2 suggested that their C termini contributed to their specificity of action. In support of this, we identified a C-terminal motif unique to PipB2, LFNEF, which dictates both its localization and biological effects. This indicates that a divergence in biological function of these two effectors can be accounted for by sequence divergence in their C termini.

MATERIALS AND METHODS

Bacterial Strains and Plasmid Constructs

The *Salmonella enterica* serovar Typhimurium strains used in this study, SL1344 wild-type, Δ*pipB* and Δ*pipB2* have been described previously (Knodler *et al*., 2002, 2003). To complement the Δ*pipB2* mutant, the *pipB2* coding sequence and ~500 base pairs of upstream promoter region was amplified from SL1344 genomic DNA with the oligonucleotides pipB2-Sal (see Table 1 for all oligonucleotide sequences) and pipB2-R-Hind. The PCR amplicon was digested with *Sal*I/*Hin*dIII and ligated into the corresponding sites of pACYC184 (~10–15 copies/cell; New England Biolabs, Beverly, MA) to create pACB2. The complementing plasmids, p*pipB-2HA*, p*pipB2-2HA*, and p*pipB2(1-225)-2HA* (all pACYC184-derivatives) encode C-terminal hemagglutinin (HA)-tagged effectors and have been described previously (Knodler *et al*., 2002, 2003). A plasmid encoding the N-terminal 312-amino acid residues of PipB2 fused to tandem HA epitopes under the control of the native *pipB2* promoter, p*pipB2*(Δ*313-350)-2HA*, was constructed as follows: a PCR fragment was amplified from SL1344 wild-type chromosomal DNA with the oligonucleotides pipB2-Sal and pipB2-312R BgI, digested with *Sal*I/*Bgl*II and cloned into the corresponding sites of p*pipB2-2HA*. Deletion of residues 341–345 of PipB2 was achieved by amplification with the oligonucleotides pipB2-Sal and PipB2-HAΔ341-345R. The amplicon was digested with *Sal*I/*Bgl*II and treated as described above for p*pipB2*(Δ*313-350)-2HA* to obtain p*pipB2*(Δ*341-345)-2HA*. Gene splicing by overlap extension (Horton *et al*., 1989) was used to replace the C-terminal 22-amino acid residues of PipB (the region distal to the pentapeptide repeat region) with the C-terminal 38-amino acid residues of PipB2 (also distal to the pentapeptide repeats). The upstream promoter region and coding sequence for the N-terminal 269 amino acids of *pipB* was amplified from p*pipB-2HA* with pipB-Sal and pipB 269R-OL. The coding sequence for amino acids 312–350 of *pipB2* and tandem C-terminal HA epitopes was amplified from p*pipB2-2HA* with the oligonucleotides pipB2 312F-OL and pipB-C3. A plasmid encoding the PipB-PipB2 fusion was created by a second round of amplification with a mix of these two amplicons and the oligonucleotides pipB-Sal and pipB-C3, followed by digestion with *Sal*I/*Hin*dIII and ligation into the corresponding sites of pACYC184 to create p*pipB-pipB2(312-350)-2HA*.

For ectopic expression studies, green fluorescent protein (GFP)-PipB2 fusions were constructed. Full-length and deletion mutants of PipB2 were amplified from SL1344 wild-type genomic DNA with the following oligonucleotides: for pGFP-PipB2, PipB2-redN1-F and PipB2-GFPC1-Hind; for pGFP-PipB2(Δ152-350), PipB2-redN1-F and EGFP-PipB2 151R; for pGFP-PipB2(Δ313-350), PipB2-redN1-F and EGFP-PipB2 312R; for pGFP-PipB2(Δ341-350), PipB2-redN1-F and GFP-PipB2 N340R; for pGFP-PipB2(Δ346-350), PipB2-redN1-F and GFP-PipB2 N345R; for pGFP-PipB2(Δ1-311), PipB2-GFPC1-312Bgl and PipB2GFPC1-Hind, and for pGFP-PipB2(Δ341-345), PipB2-redN1-F and PipB2Δ341-345-R. All PCR products were digested with *Bgl*II/*Hin*dIII and ligated into the corresponding sites of pEGFP-C1 (BD Biosciences Clontech, Palo Alto, CA). To construct pHA-PipB2, *pipB2* was amplified from SL1344 wild-type genomic DNA with the oligonucleotides pCMVHA-pipB2-F and pCMVHA-pipB2-R, the PCR product digested with *Eco*RI/*Bgl*II and ligated into the corresponding sites of pCMV-HA (BD Biosciences Clontech). pGFP-PipB2 T340A, L341A, F342A, N343A, E344A, and F345A point mutants were constructed using the QuikChange site-directed mutagenesis kit according to the manufacturer's instructions (Stratagene, La Jolla, CA). All constructs were verified by sequencing.

The following plasmids have been described previously: GFP-Rab7 Q67L (Bucci *et al*., 2000), GFP-RILP (Cantalupo *et al*., 2001), and GFP-Rab34 Q111L (Wang and Hong, 2002).

Infection and Transfection of Mammalian Cells

HeLa (human cervical adenocarcinoma, ATCC CCL-2) cells were grown at 37°C in 5% CO_2 in Eagle's minimal essential medium (Mediatech, Herndon, VA) supplemented with 10% (vol/vol) fetal bovine serum (Invitrogen, Carlsbad, CA). HeLa cells were seeded on glass coverslips in 24-well tissue culture plates 18–24 h before bacterial infections or transient transfection. Preparation of SPI-1 induced bacteria and infection conditions have been described in detail previously (Knodler *et al*., 2002). Plasmid DNA was prepared using the Perfectprep Plasmid Midi kit according to the manufacturer's instructions (Eppendorf, Boulder, CO), and transfections were with FuGENE 6 reagent (Roche Diagnostics, Indianapolis, IN).

Immunofluorescence

HeLa cells were processed for immunofluorescence at either 12 h postinfection (p.i.) or 24 h posttransfection. Monolayers were fixed in 2.5% (wt/vol) paraformaldehyde (PFA) for 10 min at 37°C, permeabilized with 0.1% (wt/

Table 1. Sequences of oligonucleotides used in this study

Oligonucleotide	Sequence (5′ to 3′)
pipB2-Sal	A CGC GTC GAC ACG GCT CTA CTA CTC GAT AG
pipB2-R-Hind	CCC AAG CTT ACT ATT CAG TAG CAG ATT GTT
pipB2–312R Bgl	GGA AGA TCT AGC CTC AGC CAA ATC AGC C
pipB2-HAΔ341-345R	GGA AGA TCT AAT ATT TTC ACT ATA TGT TTG TGT GCT TGT AGA CAT TGT
pipB-Sal	A CGC GTC GAC ATA CTT TCT TAA TGA GAT AAA ACG
pipB 269R-OL	TAA ATT AGC ACC TGT CAG ATC GGC TCC TGT
pipB2 312F-OL	CTG ACA GGT GCT AAT TTA AAC AAT ACC TGT
pipB-C3	AAG CTT GTT TAT AAA ATC CCT TTA TCT CGA
pipB2-redN1-F	GGA AGA TCT ATG GAG CGT TCA CTC GAT
pipB2-GFPC1-Hind	CCC AAG CTT CTA AAT ATT TTC ACT ATA AAA TTC
GFP-PipB2 151R	CCC AAG CTT CTA GCC TCC CTG GGC AGT TAA
GFP-PipB2 312R	CCC AAG CTT CTA AGC CTC AGC CAA ATC AGC
GFP-PipB2 N340R	CCC AAG CTT CTA TGT TTG TGT GCT TGT AGA
GFP-PipB2 N345R	CCC AAG CTT CTA AAA TTC GTT AAA GAG TGT TT
PipB2-GFPC1-312Bgl	GGG AGA TCT GCT AAT TTA AAC AAT ACC
GFP-PipB2Δ341-345R	CCC AAG CTT CTA AAT ATT TTC ACT ATA TGT TTG TGT GCT TGT AGA CAT TGT
pCMVHA-pipB2-F	CCG GAA TTC GTT CAC TCG ATA GTC TG
pCMVHA-pipB2-R	GGA AGA TCT CTA AAT ATT TTC ACT ATA AAA

Engineered restriction sites are underlined.

vol) saponin, and immunostained as described previously (Knodler *et al*., 2003). Alternatively, where stated, monolayers were fixed in −20 °C methanol for 1 min. Primary antibodies and dilutions used were rabbit α-*Salmonella* lipopolysaccharide (LPS), 1:2000 (Difco, Detroit, MI); mouse α-*Salmonella* LPS, 1:5000 (Biodesign International, Saco, ME); mouse α-human LAMP-1, 1:100 (H4A3; developed by J. T. August and obtained from the Developmental Studies Hybridoma Bank developed under the auspices of the National Institute of Child Health and Human Development and maintained by the Department of Biological Sciences, University of Iowa, Iowa City, IA); rabbit α-LAMP-2, 1:1000 (courtesy of Minoru Fukuda, The Burnham Institute, La Jolla, CA) (Carlsson *et al*., 1988); mouse α-LBPA, 1:50 (clone 6C4; courtesy of Jean Gruenberg, University of Geneva, Switzerland); rat α-HA high-affinity, 1:250 (clone 3F10; Roche Applied Science, Indianapolis, IN); mouse α-HA.11, 1:2000 (clone 16B12; Covance, Berkeley, CA); rabbit α-cathepsin D, 1:250 (courtesy of Walter Gregory and Stuart Kornfeld, Washington University School of Medicine, St. Louis, MO); mouse α-early endosome antigen-1 (EEA-1), 1:100 (clone 14; BD Transduction Laboratories, Lexington, KY), mouse α-β-tubulin, 1:50 (Sigma, St. Louis, MO), and sheep α-*trans*-Golgi network 46 (TGN46), 1:100 (methanol fixation) (Serotec, Oxford, United Kingdom). Alexa Fluor 488- and Alexa Fluor 568-labeled secondary antibodies were used at a dilution of 1:800 (Molecular Probes, Eugene, OR). Cy5-labeled secondary antibodies were used at a dilution of 1:600–1:800 (Jackson ImmunoResearch Laboratories, West Grove, PA). Mammalian and bacterial DNA was labeled with DRAQ5 (Biostatus, Shepshed, Leicestershire, United Kingdom).

For functional analysis of the redistributed organelles, HeLa cells were transfected with pGFP-PipB2 for 12 h and then incubated with 130 μg/ml Alexa Fluor 568-conjugated dextran, 10,000 mol. wt. (Molecular Probes) overnight in culture medium, washed, and incubated for 1 h in dextran-free media. Monolayers were fixed in PFA and examined by confocal microscopy. Alternatively, HeLa cells were incubated with 50 nM LysoTracker Red DND-99 (Molecular Probes) in culture medium for 2 h before fixation with PFA as described above. To depolymerize microtubules, HeLa cells were treated with 5 μg/ml nocodazole (NDZ) (Sigma) for 30 min at 37°C.

Confocal Microscopy Analysis

For confocal fluorescence microscopy, we used a modified PerkinElmer UltraView spinning disk confocal system connected to a Nikon Eclipse TE2000-S microscope with a 60× Plan-Apo oil immersion objective (numerical aperture 1.4; Nikon, Tokyo, Japan). The system was fitted with a Laser Launcher (Prairie Technologies, Middleton, WI) with two lasers, krypton argon (488 line) and argon (568 and 647 lines), and an acoustic optical tunable filter for wavelength selection. A Photometrics Cascade:512F camera (Roper Scientific, Trenton, NJ) was used for data acquisition. For fixed samples, eight to 10 confocal sections (0.2-μm steps) were acquired and assembled into flat projections using ImageJ or MetaMorph software (Universal Imaging, Downingtown, PA). Adobe Photoshop was used to assemble images into final figures. For live cell imaging, cells seeded in 0.17-mm Delta T dishes (Bioptechs, Butler, PA) were maintained in phenol-red free Dulbecco's minimal essential medium (Mediatech) containing 10 mM HEPES, 1.6 mM $NaHCO_3$, and 0.2% (wt/vol) bovine serum albumin during observation. Images were converted into QuickTime movies using Volocity (Improvision, Coventry, United Kingdom).

The "Sif extension index" measures the fraction of the total microtubule area covered by Sifs. A similar method has been used previously to measure tubular lysosome extension along microtubules in macrophages (Hollenbeck and Swanson, 1990). To calculate the Sif extension index, blind conditions were used and single confocal sections of randomly chosen Sif-positive infected cells (12 h p.i., stained with LAMP-2, β-tubulin, and DRAQ5) were taken. Using MetaMorph software, the total microtubule area for each cell was determined after defining the perimeter of β-tubulin staining (see Figure 1 for example, continuous line). To measure Sif extension, the perimeter of the outermost point of all LAMP-2 decorated Sifs was drawn (see Figure 1 for example, dotted line) and the encompassing area was calculated. The LAMP-2 area was divided by the β-tubulin area and multiplied by 100 to give a percentage that represents the Sif extension index. With this scoring method, the farther that Sifs extend away from the juxtanuclear SCV toward the cell periphery, the larger the LAMP-2/β-tubulin ratio and the larger the Sif extension index.

Cell fractionation

HeLa cells were seeded in 10-cm dishes, transfected 18–24 h later, and then subject to mechanical fractionation at 24 h posttransfection. Mechanical fractionation was performed as described previously (Knodler *et al*., 2003), except that the low-speed centrifugation step was at 3000 × *g*. The three fractions obtained were nuclei, cytoskeleton, and unbroken cells (P); cell membranes (M); and cytoplasm (C).

Immunoblotting

Proteins were separated on SDS-PAGE gels and transferred to nitrocellulose (Bio-Rad, Hercules, CA). Membranes were blocked for 2 h at room temperature in Tris-buffered saline with 0.1% (vol/vol) Tween 20 and 5% (wt/vol) milk powder (TBST-milk), then incubated overnight at 4°C in TBST-milk with the following primary antibodies: rabbit α-GFP, 1:50,000 (Molecular Probes); rabbit α-calnexin carboxy terminus, 1:50,000 (StressGen Biotechnologies, San Diego, CA); and mouse α-Hsp27, 1:5000 (clone G31; Cell Signaling Technology, Beverly, CA). Incubation with secondary antibodies peroxidase-conjugated goat α-rabbit or α-mouse IgG, 1:10,000 (Cell Signaling Technology) was in TBST-milk at room temperature for 1 h. SuperSignal West Femto Maximum Sensitivity substrate (Pierce Chemical, Rockford, IL) was used for chemiluminescent detection.

Statistical Analyses

All experiments were repeated at least three times. Geometric means were determined and one-way analysis of variance (ANOVA) followed by a Dunnett's multiple comparison was performed. A p value of <0.01 was considered significant.

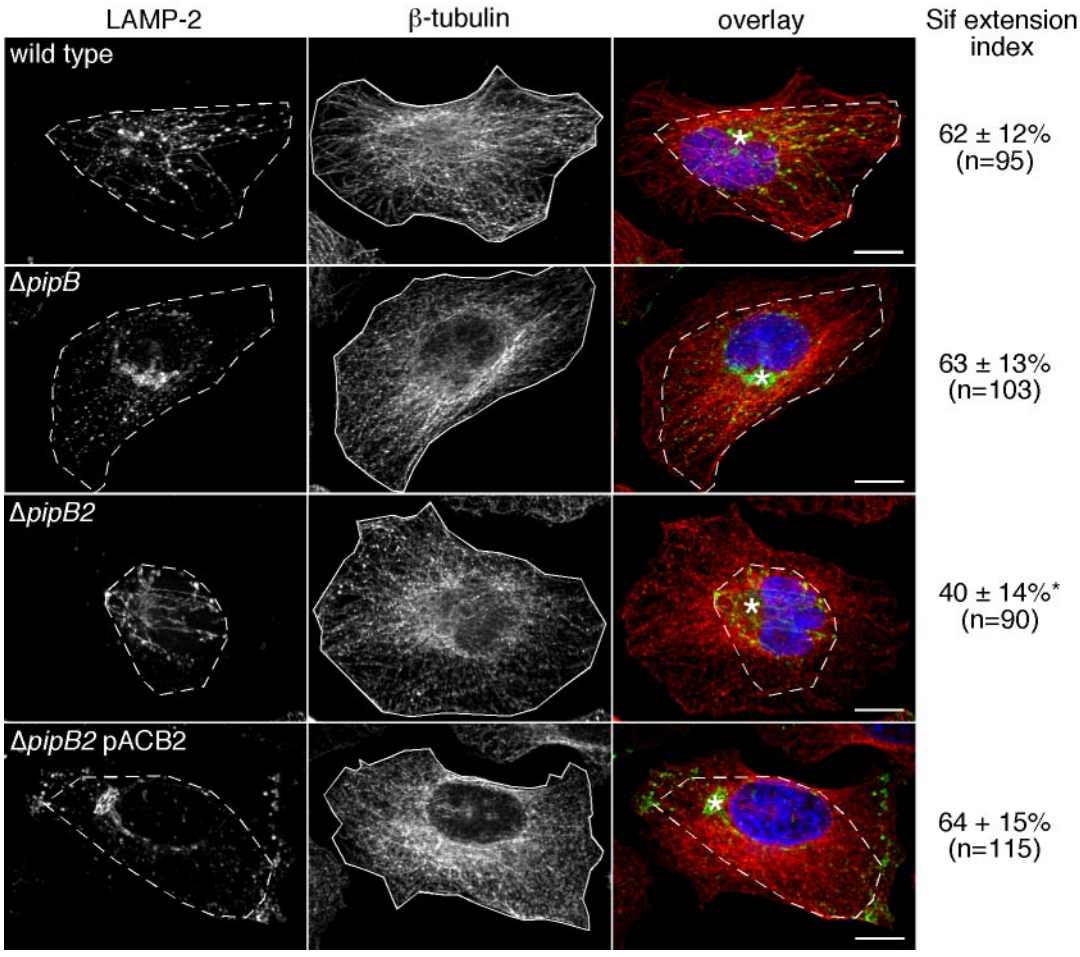

Figure 1. PipB2 is required for the centrifugal extension of Sifs. HeLa cells were infected with the indicated bacteria; SL1344 wild-type, Δ*pipB*, Δ*pipB2*, or Δ*pipB2* complemented in trans with PipB2 (Δ*pipB2* pACB2). At 12 h p.i., monolayers were fixed, permeabilized, and stained for LE/Lys (LAMP-2; green in overlay), microtubules (β-tubulin; red) and bacterial and host cell DNA (DRAQ5; blue). Confocal images of randomly chosen Sif-containing infected cells were taken. Example images for each infection condition are shown. For each cell, the Sif extension index was measured as described in *Materials and Methods*. This is a measure of the radial extension of Sifs along microtubules, i.e., the farther that Sifs extend outwards from the juxtanuclear SCV, toward the cell periphery, the larger the Sif extension index. Dashed lines and solid lines indicate the area covered by the Sif network and microtubules, respectively, in each cell. Results are the mean ± SD from three separate experiments. Data significantly different from wild-type infection is indicated by an asterisk ($p < 0.001$). The total number of Sif-positive infected cells scored is indicated. Asterisks on overlay indicate SCV positioning. Bar, 10 μm.

RESULTS

PipB2 Is Required for the Centrifugal Extension of Sifs

Given that the SPI-2 TTSS mediates postinvasion host cell interactions, including SCV and Sif biogenesis (Waterman and Holden, 2003; Kuhle and Hensel, 2004), we hypothesized that PipB and PipB2 may contribute to the formation or maintenance of these structures in infected cells. To test this, we infected HeLa cells with wild-type, Δ*pipB*, or Δ*pipB2* bacteria and then assessed SCV membrane integrity and Sif formation by confocal microscopy. Infected cells were fixed at 12 h p.i., which coincides with the peak of Sif formation in epithelial cells (Birmingham *et al*., 2005), and immunostained for the LE/Lys marker LAMP-2 to detect SCV and Sifs and LPS, to detect bacteria. We found that PipB and PipB2 are not required for LAMP-1 accumulation around bacteria or Sif frequency (Table 2), confirming our previous observations from 9 h p.i. (Knodler *et al*., 2003). However, the Sifs in Δ*pipB2*-infected cells seemed shorter than those in cells infected with wild-type or Δ*pipB* bacteria (Figure 1). To evaluate this phenotype, we devised a scoring method whereby the area occupied by the Sif network (LAMP-2 staining, shown as dashed line in Figure 1) is expressed as a percentage of the total cell area (β-tubulin staining, shown as continuous line in Figure 1). This Sif extension index measures the radial extension of Sifs along microtubules for each infected cell and is less susceptible to the bias and variability introduced when measuring individual Sif-tubule length. Using this scoring method, the Sifs formed in cells infected with wild-type or Δ*pipB* bacteria were indistinguishable; Sif extension indices were 62 ± 12% for wild-type (n = 95) and 63 ± 13% for Δ*pipB* (n = 103) (Figure 1). In contrast, Sifs in Δ*pipB2*-infected cells occupied significantly less of the HeLa cell area, with a Sif extension index of 40 ± 14% (n = 90) (Figure 1; $p < 0.001$). Complementation of the Δ*pipB2* mutant with plasmid-borne PipB2 restored the index of Sif extension to wild-type levels (64 ± 15%; Figure 1). Thus, both qualitatively and quantitatively, PipB2 is required for the centrifugal extension of Sifs away from the SCV.

Table 2. In trans complementation of a Δ*pipB2* mutant increases LAMP-1 accumulation at the cell periphery and decreases Sif frequency in infected cells

Strain	Peripheral LAMP-1-positive vesicles (%)	Sif-positive cells (%)	LAMP-1-positive bacteria (%)
SL1344 wild type	7.0 ± 3.5	62 ± 3.9	90 ± 3.5
Δ*pipB2*	5.7 ± 3.0	57 ± 6.2	91 ± 3.0
Δ*pipB2* PipB2–2HA	46 ± 12*	44 ± 5.7*	94 ± 3.0
Δ*pipB2* PipB2(1–225)-2HA	8.7 ± 3.8	60 ± 3.9	
Δ*pipB2* PipB2(Δ313-350)-2HA	7.0 ± 4.7	60 ± 4.8	
Δ*pipB2* PipB2(Δ341-345)-2HA	11 ± 1.2	62 ± 4.7	93 ± 5.2
Δ*pipB2* pACYC184	5.0 ± 3.7	62 ± 3.2	94 ± 3.1
Δ*pipB*	4.8 ± 1.2	63 ± 4.2	93 ± 4.1
Δ*pipB* PipB-2HA	9.9 ± 4.0	58 ± 3.2	92 ± 2.1
Δ*pipB* PipB-PipB2(312-350)-2HA	9.2 ± 3.4	60 ± 5.6	

HeLa cells were seeded on coverslips in 24-well plates and infected with late-log phase bacteria as described in *Materials and Methods*. At 12 h postinfection, monolayers were fixed, permeabilized, and immunostained with anti-*Salmonella* LPS and anti-human LAMP-1 antibodies. Infected cells (>100 per experiment) were scored by fluorescent microscopy for LAMP-1 accumulation at the cell periphery, LAMP-1 accumulation around bacteria, and the presence of linear or punctate LAMP-1 staining extending from SCVs (a measure of Sif formation). Results are mean ± SD from at least three independent experiments.

* Statistically different from wild type infection, $p < 0.001$, ANOVA.

In Trans Complementation of a ΔpipB2 Mutant Reduces Sif Frequency

Epitope-tagged effectors translated from low copy number plasmids have been successfully used to monitor type III translocation and subsequent intracellular localization of these proteins (Knodler *et al*., 2002, 2003; Kuhle and Hensel, 2002; Brumell *et al*., 2003; Freeman *et al*., 2003). Here, we have used C-terminally HA-tagged effectors to further characterize the role of PipB2 in Sif formation. HeLa cells were infected with *Salmonella* expressing either p*pipB-2HA* or p*pipB2-2HA*, fixed at 12 h p.i., and processed for immunofluorescence microscopy using antibodies against the HA tag, *Salmonella* LPS and the LE/Lys glycoprotein LAMP-1. Figure 2A shows that both PipB and PipB2 localized to the SCV and Sifs, although the Sifs formed in the presence of PipB2-2HA were notably less complex. PipB2 also localized to tubular-vesicular structures that collected at the extreme cell periphery, particularly in regions of membrane protrusions (Figure 2A, arrowheads). Strikingly, LAMP-1 also was redistributed to these peripheral regions (Figure 2A and Table 2). Although PipB2 and LAMP-1 both localized to the cell periphery, only partial colocalization was observed for these proteins (Figure 2A). Despite the peripheral accumulation of LAMP-1 in Δ*pipB2* p*pipB2-2HA*-infected cells, LAMP-1 accumulation around bacteria (Table 2) and juxtanuclear SCV positioning (Figure 2A) seemed unaffected.

Because type III translocation of PipB2-2HA induced an accumulation of LE/Lys compartments at the cell periphery (Table 2), and reduced Sif complexity (Figure 2A), we next assessed whether the frequency of Sif formation also was affected. Table 2 shows that in trans complementation of the Δ*pipB2* mutant with p*pipB2-2HA* significantly reduced Sif frequency compared with Δ*pipB2* or wild-type bacteria ($p < 0.001$). Evidently, the multicopy nature of p*pipB2-2HA* results in an increased synthesis and translocation of PipB2-2HA compared with chromosomal *pipB2* in wild-type bacteria, a feature previously noted for plasmid-borne expression of other effectors (Cain *et al*., 2004; Drecktrah *et al*., 2005). Accordingly, because we observe that deletion of *pipB2* inhibits the centrifugal extension of Sifs and bacterial overexpression of *pipB2-2HA* causes the accumulation of LE/Lys at the cell periphery, we conclude that PipB2 is involved in the movement of these lgp-rich tubules, away from the SCV, toward the cell periphery.

The C-Terminal 38 Residues of PipB2 Are Required for Targeting to the Cell Periphery and Redistribution of LAMP-1

We next considered which region(s) of PipB2 were responsible for its localization to the periphery and ability to redistribute LAMP-positive compartments. By comparing the deduced amino acid sequences of PipB and PipB2 (see Knodler *et al*., 2003 for sequence alignment), we predicted that differences in the localization of these two proteins were due to their highly divergent C termini. To address this hypothesis, we engineered a truncated PipB2 construct, PipB2(Δ313-350)-2HA, in which the unique C-terminal 38-amino acid residues of PipB2 were deleted. HeLa cells were infected for 12 h with Δ*pipB2* p*pipB2(Δ313-350)-2HA* bacteria and processed for immunofluorescence. As predicted, PipB2(Δ313-350)-2HA did not localize to peripheral vesicles like full-length PipB2-2HA but instead had a localization pattern like that of PipB-2HA (compare Figure 2, A and B) and another PipB2 truncation, PipB2(1-225)-2HA (Knodler *et al*., 2003). Furthermore, PipB2(Δ313-350)-2HA did not induce the redistribution of LAMP-1-positive compartments or decrease Sif frequency (Figure 2B and Table 2). We conclude that the C-terminal 38-amino acid residues of PipB2 are essential for its peripheral targeting and reorganization of LAMP-positive compartments.

We next considered whether replacing the C-terminal 22 residues of PipB with the C-terminal 38 residues of PipB2 would be sufficient to localize PipB and/or LAMP-positive compartments to the cell periphery. HeLa cells were infected with Δ*pipB* p*pipB-pipB2(312-350)-2HA* bacteria and immunostained as described above. However, the intracellular distribution of the translocated PipB-PipB2 chimera was indistinguishable from that of PipB (compare Figure 2, A and B) and LAMP-1-positive compartments were not redistributed to the cell periphery (Figure 2B and Table 2). We conclude that peripheral localization of translocated PipB2 and its effects on LE/Lys are dependent on the C-terminal 38-amino acid residues, although other regions of PipB2 must also contribute targeting information.

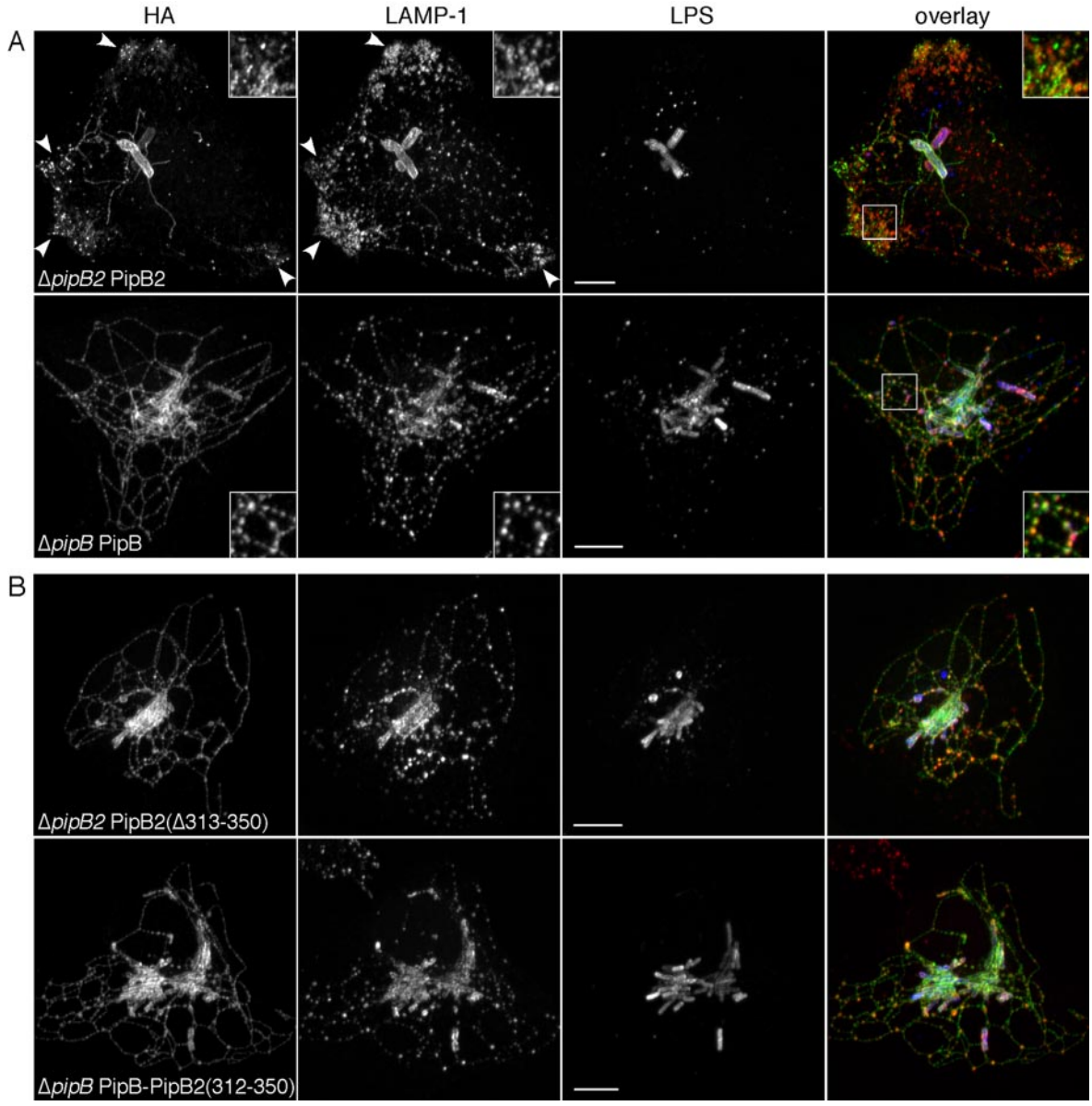

Figure 2. The C-terminal 38-amino acid residues of PipB2 are required for its unique peripheral localization and effect on LE/Lys. HeLa cells were infected with Δ*pipB2* p*pipB2-2HA* (A, top) or Δ*pipB* p*pipB-2HA* bacteria (A, bottom), or Δ*pipB2* p*pipB2*(Δ*313-350)-2HA* (B, top) or Δ*pipB* p*pipB-pipB2(312-350)-2HA* (B, bottom) bacteria. At 12 h p.i., monolayers were fixed, permeabilized, and immunostained for HA-tagged PipB or PipB2, LAMP-1, and *Salmonella* LPS. Samples were viewed by confocal microscopy. An overlay of the three channels is presented on the right (HA-tagged effectors, green; LAMP-1, red; and LPS, blue). Inset shows 2× enlargement of boxed area. Arrowheads indicate PipB2-2HA and LAMP-1 accumulation at the cell periphery. Bar, 10 μm.

Ectopically Expressed PipB2 Redistributes LE/Lys

Our studies of translocated PipB2-2HA indicated a role for PipB2 in LE/Lys organization and Sif extension. We speculated that if a similar phenotype was observed upon ectopic expression of PipB2 in mammalian cells, we could use this approach to study the biological properties of PipB2 without the interference of other SPI-2 effector activities. HeLa cells were transfected with a plasmid encoding PipB2 tagged at the N terminus with GFP (pGFP-PipB2) and examined by confocal microscopy for localization and effects on LE/Lys positioning. In a pattern similar to that seen for bacterially translocated PipB2-2HA (Figure 2A; Knodler *et al*., 2003), peripheral accumulation of GFP-PipB2 was detected by 24 h (Figure 3). This concentration was toward the basal surface, near where cells attached to the coverslip, and predominantly at sites of membrane projections. GFP-PipB2 also associated with vesicular-tubular structures that extended from the perinuclear area to the cell periphery. The characteristic steady-state distribution of LE/Lys was dramatically affected by pGFP-PipB2 expression. In the majority of cells expressing GFP-PipB2, LE/Lys compartments shifted to the cell periphery (Figures 3–6). In comparison, LE/Lys in untransfected cells is predominantly perinuclear. This effect was specific to GFP-PipB2 because cells transfected with GFP-PipB or GFP alone showed normal LE/Lys distribution (our unpublished data). GFP-PipB2 also partially colocalized with markers for LE/Lys compartments, such as LAMP-1, cathepsin D, LBPA (Figure 3, A–C), LAMP-2 and LAMP-3

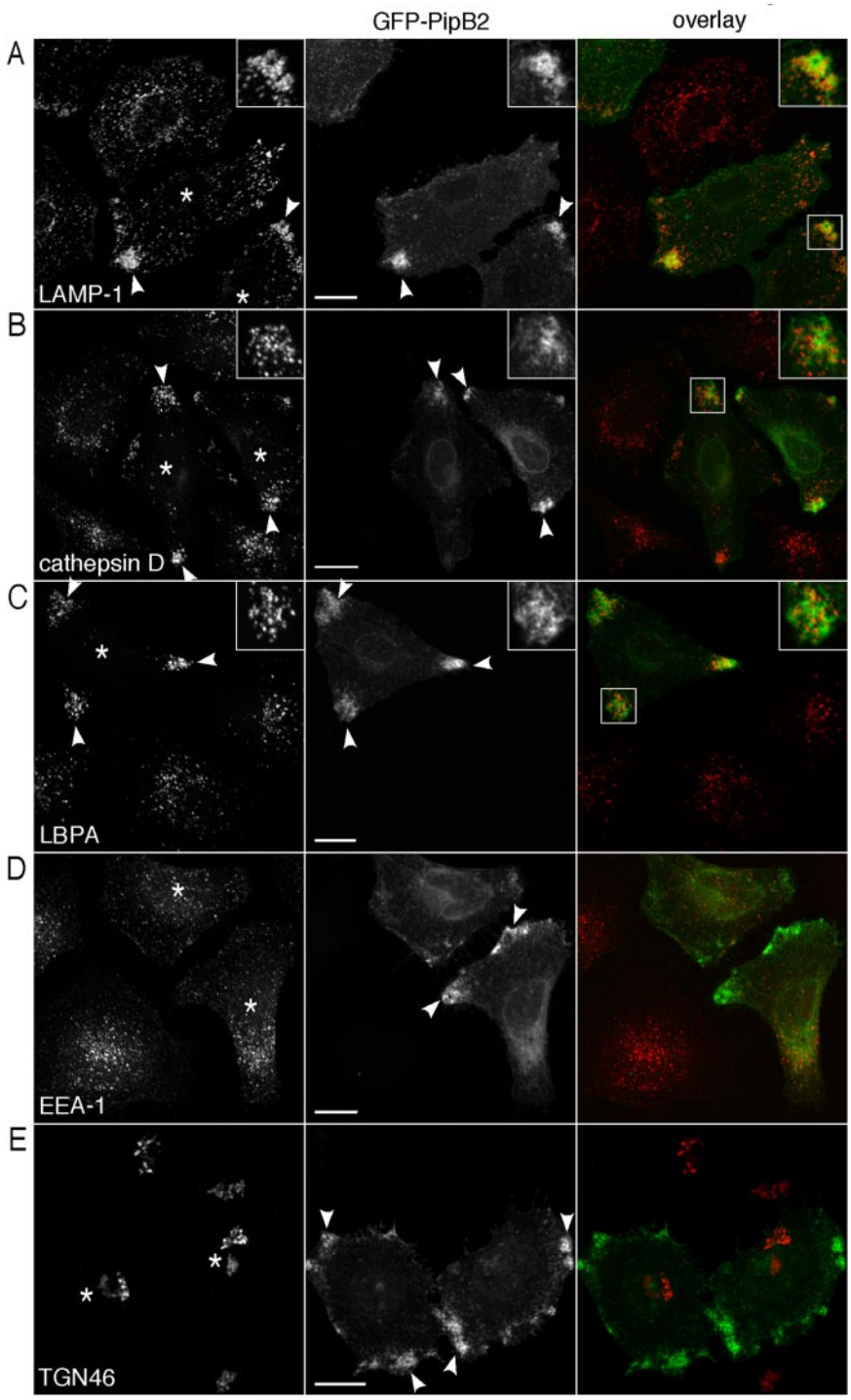

Figure 3. Ectopic expression of PipB2 induces the redistribution of LE/Lys, but not other organelles, to the extreme cell periphery. HeLa cells were transiently transfected with pGFP-PipB2 and processed for immunofluorescence 24 h later using antibodies against LAMP-1 (LE/Lys glycoprotein) (A), cathepsin D (lysosomal enzyme) (B), LBPA (late-endosome specific lipid) (C), EEA-1 (early endosomes) (D), and TGN46 (*trans*-Golgi network marker) (E). Samples were viewed by confocal microscopy. An overlay of the two channels is presented on the right (GFP-PipB2, green; and organelle marker, red). Insets show 2× enlargement of boxed area. Asterisks indicate transfected cells and arrowheads indicate peripheral accumulation of GFP-PipB2 and/or LE/Lys. Bar, 20 μm.

(LIMP-1/CD63) (our unpublished data). The steady-state distribution of other organelles, including early endosomes (EEA-1, Figure 3D), *trans*-Golgi network (TGN46, Figure 3E), Golgi apparatus (p115; our unpublished data), and endoplasmic reticulum (calnexin; our unpublished data) was not affected by GFP-PipB2. We conclude from these results that, in HeLa cells, ectopic expression of GFP-PipB2 duplicates the biological properties of bacterially translocated PipB2-2HA, namely, localizing to the cell periphery and inducing the peripheral accumulation of LE/Lys compartments.

Cotransfection Studies to Analyze the Mechanism of Action of PipB2

Overexpression of mammalian proteins involved in the steady-state positioning of organelles can perturb their cellular localization. For example, overexpression of Rab7, Rab34, or RILP increases the perinuclear clustering of LE/Lys, the opposite effect of GFP-PipB2. However, like for PipB2, the spatial positioning of other organelles are not affected (Cantalupo *et al*., 2001; Jordens *et al*., 2001; Wang *et al*., 2004). Rab7 and RILP also are required for SCV biogen-

esis and Sif formation (Méresse *et al*., 1999; Brumell *et al*., 2001; Jordens *et al*., 2001; Harrison *et al*., 2004). To dissect the mechanism of action of PipB2 on LE/Lys distribution, we coexpressed HA-PipB2 with these three mammalian proteins; dominant-active Rab7 (GFP-Rab7 Q67L), dominant-active Rab34 (GFP-Rab34 Q111L) or RILP and examined the distribution of LE/Lys in HeLa cells. Transfected monolayers were immunostained with LAMP-2 to label LE/Lys and α-HA antibodies to detect HA-PipB2. In agreement with previous observations (Bucci *et al*., 2000), overexpression of GFP-Rab7 Q67L increased the perinuclear accumulation of LE/Lys (Figure 4A, bottom, LAMP-2). However, HA-PipB2 was able to overcome the effects of GFP-Rab7 Q67L because PipB2, Rab7 Q67L and LAMP-2 all accumulated at the periphery in cotransfected cells (Figure 4A, top). Rab34, like Rab7, binds to RILP to control LE/Lys positioning (Cantalupo *et al*., 2001; Jordens *et al*., 2001; Wang and Hong, 2002) but is primarily Golgi-associated and regulates LE/Lys distribution in trans (Wang and Hong, 2002). An enhanced perinuclear accumulation of LE/Lys was observed in cells overexpressing GFP-Rab34 Q111L (Figure 4B, bottom) (Wang and Hong, 2002). However, when HeLa cells were cotransfected with HA-PipB2, both LE/Lys and PipB2 shifted to the periphery, demonstrating that PipB2 is dominant over Rab34 with respect to LE/Lys positioning (Figure 4B, top). Notably, the Golgi association of GFP-Rab34 Q111L was unaffected by PipB2 expression (Figure 4B, top), confirming that the effects of PipB2 are restricted to LE/Lys positioning. RILP overexpression induces a much higher degree of LE/Lys clustering compared with Rab7 Q67L or Rab34 Q111L (Cantalupo *et al*., 2001; Jordens *et al*., 2001) (Figure 4C, bottom). We found that PipB2 could partially overcome the effects of RILP expression. Coexpression of GFP-RILP and HA-PipB2 caused an intermediate phenotype where the actions of neither RILP nor PipB2 dominated. GFP-RILP positive structures became more dispersed, HA-PipB2 no longer displayed a strong peripheral accumulation and LE/Lys seemed to be scattered throughout the cytoplasm (Figure 4C, top). Collectively, the coexpression data show that the actions of PipB2 are dominant over both Rab7 and Rab34 but not RILP. Therefore PipB2 is either acting downstream of Rab7 and Rab34, or in a parallel pathway, to regulate LE/Lys positioning. With regards to RILP, a number of possible conclusions can be drawn. The effects of RILP overexpression may be too potent for PipB2 to completely overcome, the actions of PipB2 and RILP may directly counteract each other or they could be acting on parallel but convergent pathways.

The Redistributed LE/Lys Remain Functional and Require Microtubules for Their Positioning

The bidirectional movement of vesicles throughout the cell and maintenance of organelle positioning is dependent on cytoskeletal "tracks" provided by microtubules and microfilaments. In nonpolarized epithelial cells, microtubules extend outwards from the microtubule organizing center (MTOC) with the fast growing "plus" ends oriented toward the cell periphery (Lane and Allan, 1998) whereas microfilaments are more randomly organized (Mallik and Gross, 2004). Microtubules are required for the localization of type III translocated PipB2-2HA (Knodler *et al*., 2003) and Sif formation (Garcia-del Portillo *et al*., 1993; Brumell *et al*., 2002). We therefore investigated whether they also were required for the peripheral localization of GFP-PipB2 and LE/Lys redistribution. HeLa cells were transfected with pGFP-PipB2 for 24 h and either left untreated or treated for 30 min with the microtubule-depolymerizing agent NDZ, followed by immunostaining with antibodies against LAMP-2 and β-tubulin. In untreated cells, GFP-PipB2 and redistributed LE/Lys collected at peripheral regions with a high concentration of microtubule plus ends (Figure 5A, top). NDZ treatment effectively depolymerized microtubules and also caused the retraction of GFP-PipB2-positive structures and LE/Lys toward the perinuclear region (Figure 5A, compare top and bottom panels). In NDZ-treated cells, we also observed extensive colocalization between GFP-PipB2 and LAMP-2 (Figure 5A, bottom). In contrast, depolymerization of actin microfilaments by cytochalasin D treatment had no effect on the peripheral accumulation of LE/Lys or GFP-PipB2 (our unpublished data). We conclude that an intact microtubule network is essential for the maintenance of GFP-PipB2 and redistributed LE/Lys at the cell periphery.

The endosomal system is composed of spatially and biochemically distinct organelles that are connected by a highly regulated membrane transport system. Spatial perturbation of this network, such as the repositioning of LE/Lys, can affect the functionality of the endocytic pathway. For example, overexpression of Rabring7 or dominant-negative Rab7 (Rab7 T22N or Rab7 N125I) affects both LE/Lys positioning and functions (Press *et al*., 1998; Bucci *et al*., 2000; Mizuno *et al*., 2003). However, overexpression of mVps18p, Vam6p/Vps39p, or dominant-active Rab34 (Rab34 Q111L) alters LE/Lys morphology but not functioning (Caplan *et al*., 2001; Wang and Hong, 2002; Poupon *et al*., 2003). We analyzed the effect of GFP-PipB2 on trafficking to LE/Lys and endosomal acidification. To follow endocytic delivery to LE/Lys, GFP-PipB2 transfected HeLa cells were incubated overnight with fluorescent dextran, a fluid phase marker; washed; and chased for 1 h to label LE/Lys. In untransfected cells, dextran was clustered in the perinuclear region (Figure 5B, Movie). In comparison, GFP-PipB2-positive cells accumulated fluorescent dextran at the periphery (Figure 5B, Movie). The cell-permeant acidotropic probe LysoTracker Red DND-99, which fluoresces within acidic compartments, also accumulated in the redistributed LE/Lys (our unpublished data). Together, these data indicate that GFP-PipB2 does not dramatically alter the accessibility of LE/Lys to fluid phase markers or their luminal pH.

Identification of Functional Domains of PipB2

Mammalian proteins that regulate vesicular trafficking are membrane associated, either stably or transiently. By analogy, PipB2 also should be membrane associated to affect LE/Lys positioning. Bacterially translocated PipB2-2HA associates with host cell membranes (Knodler *et al*., 2003) and ectopically expressed PipB2-labeled vesicular-tubular structures (Figures 3–5, Movie). To confirm the subcellular targeting of GFP-PipB2 and identify targeting domains, HeLa cells were transiently transfected with pGFP-PipB2 or the deletion constructs pGFP-PipB2(Δ313-350), pGFP-PipB2(Δ152-350), or pGFP-PipB2(Δ1-311) (depicted in Figure 6A) and then mechanically disrupted after 24 h. Separation by consecutive low- and high-speed centrifugations produced three fractions; nuclei, cytoskeleton, and unbroken cells (P); cell membranes (M); and cytosol (C), equal volumes of which were analyzed by immunoblotting for GFP-PipB2 fusions, calnexin (membrane marker) and Hsp27 (cytosolic marker) (Figure 6B). GFP-PipB2 and GFP-PipB2(Δ313-350) were both detected in P and M fractions. GFP fused to the N-terminal 151 residues of PipB2, pGFP-PipB2(Δ152-350), partitioned in all three

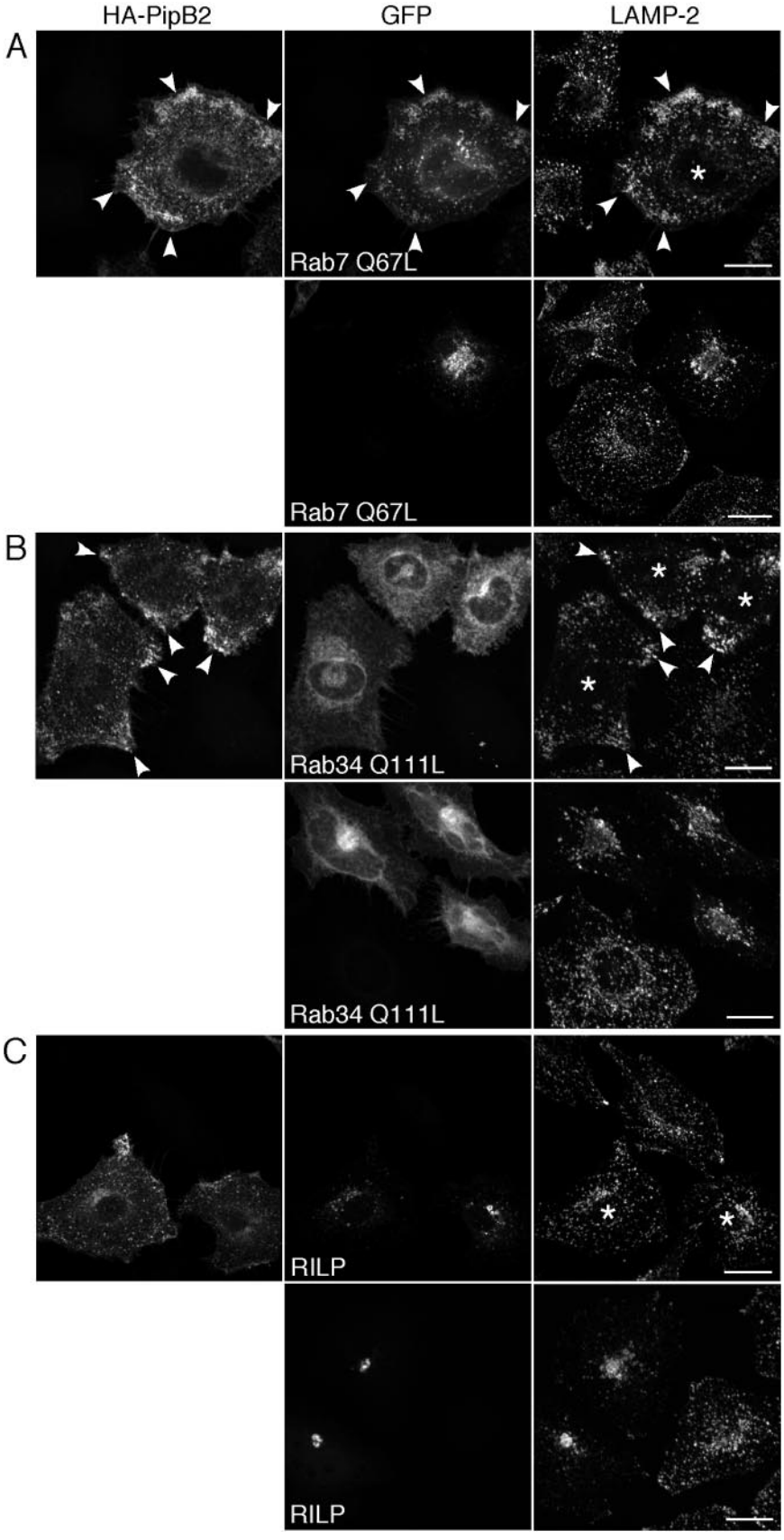

Figure 4. Effects of PipB2 dominate over those of Rab7 and Rab34, but not RILP, with respect to LE/Lys positioning. HeLa cells were transiently transfected with either: (A) GFP-Rab7 Q67L alone (bottom) or GFP-Rab7 Q67L and HA-PipB2 (top). (B) GFP-Rab34 Q111L alone (bottom) or GFP-Rab34 Q111L and HA-PipB2 (top). (C) GFP-RILP alone (bottom) or GFP-RILP and HA-PipB2 (top). Monolayers were fixed and processed for immunofluorescence 24 h later using α-HA antibodies to detect HA-PipB2 and α-LAMP-2 to detect LE/Lys. Asterisks indicate HeLa cells transfected with both plasmids. Arrowheads indicate peripheral accumulation of HA-PipB2 and LE/Lys in cotransfected cells. Bar, 20 μm.

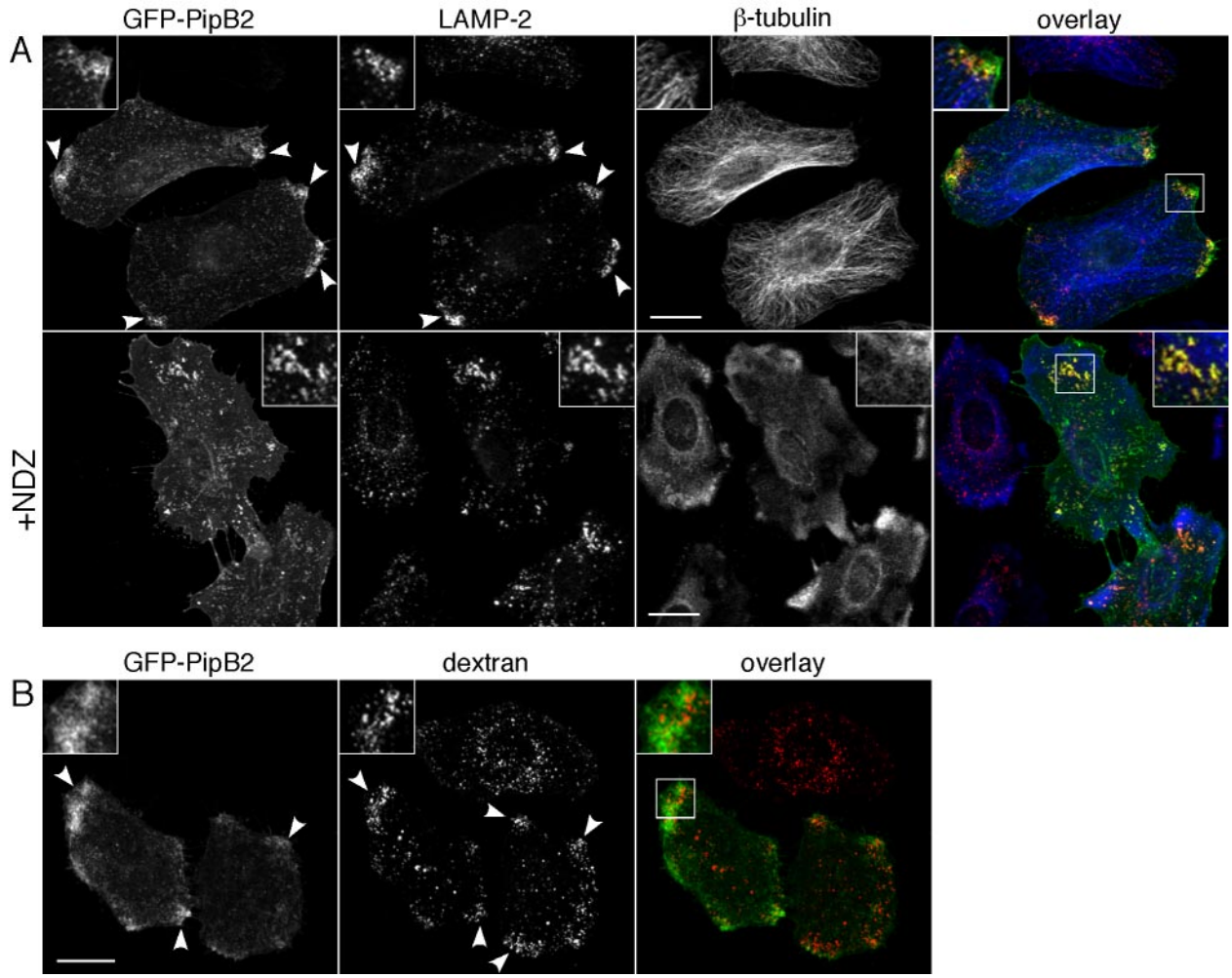

Figure 5. Functionality of the redistributed LE/Lys. (A) Positioning of GFP-PipB2 and redistributed LE/Lys requires an intact microtubule network. HeLa cells were transiently transfected with pGFP-PipB2 for 24 h and either left untreated (top) or treated with 5 μg/ml NDZ for 30 min (+NDZ, bottom). Monolayers were fixed, permeabilized, and immunostained for β-tubulin and LAMP-2 and viewed by confocal microscopy. An overlay of the three channels is presented on the right (GFP-PipB2, green; β-tubulin, blue; and LAMP-2, red). Insets show 2× enlargement of boxed area. Arrowheads indicate peripheral accumulation of GFP-PipB2 and LAMP-2. Bar, 20 μm. (B) The redistributed LE/Lys are accessible to fluid phase markers. HeLa cells were transiently transfected with pGFP-PipB2 and then incubated for 12 h with 130 μg/ml Alexa Fluor 568-labeled dextran, washed, and further incubated in dextran-free medium for 1 h to label LE/Lys. Monolayers were fixed and examined by confocal microscopy. Arrowheads indicate peripheral accumulation of dextran and GFP-PipB2 in transfected cells. An overlay of the two channels is shown on the right (GFP-PipB2, green; and dextran, red). Insets show 2× enlargement of boxed area. Bar, 20 μm.

fractions, whereas GFP fused to the C-terminal 38-amino acid residues of PipB2 was predominantly cytosolic. Together, a number of conclusions can be drawn from this data. First, PipB2 is stably associated with cell membranes when ectopically expressed indicating that interaction with other *Salmonella* effectors is not required for its membrane association. Second, whereas the N-terminal 151 amino acid residues of PipB2 are sufficient to confer membrane targeting, additional residues are required for absolute membrane association. This agrees with our previous delineation of the N-terminal 225 residues as being sufficient for host cell membrane association after type III translocation (Knodler *et al*., 2003). Finally, the C-terminal 38 residues of PipB2 do not impart membrane association when fused to GFP.

Type III translocation studies indicated that the C-terminal 38 residues of PipB2 are required for its biological activity on LE/Lys. To confirm and extend this definition of PipB2 sequence requirements, we transiently transfected HeLa cells with a series of GFP-tagged PipB2 truncations (depicted in Figure 6A) and determined their ability to redistribute LE/Lys by immunofluorescence microscopy (Figure 6C). Removing five amino acid residues from the C terminus of PipB2 [pGFP-PipB2(Δ346-350)] did not prevent its peripheral targeting or LE/Lys redistribution properties. However, constructs bearing further C-terminal deletions (pGFP-PipB2(Δ341-350), pGFP-PipB2(Δ313-350), and pGFP-PipB2(Δ152-350) did not redistribute LAMP-1 (Figure 6, C and D) or localize to the cell periphery (Figure 6D). Instead, these truncated PipB2 proteins accumulated in the perinuclear region [pGFP-PipB2(Δ341-350)] or associated with membranous structures throughout the cell [pGFP-PipB2(Δ152-350) and pGFP-PipB2(Δ313-350)]. Finally, a construct consisting of the C-terminal 38 amino acids of PipB2

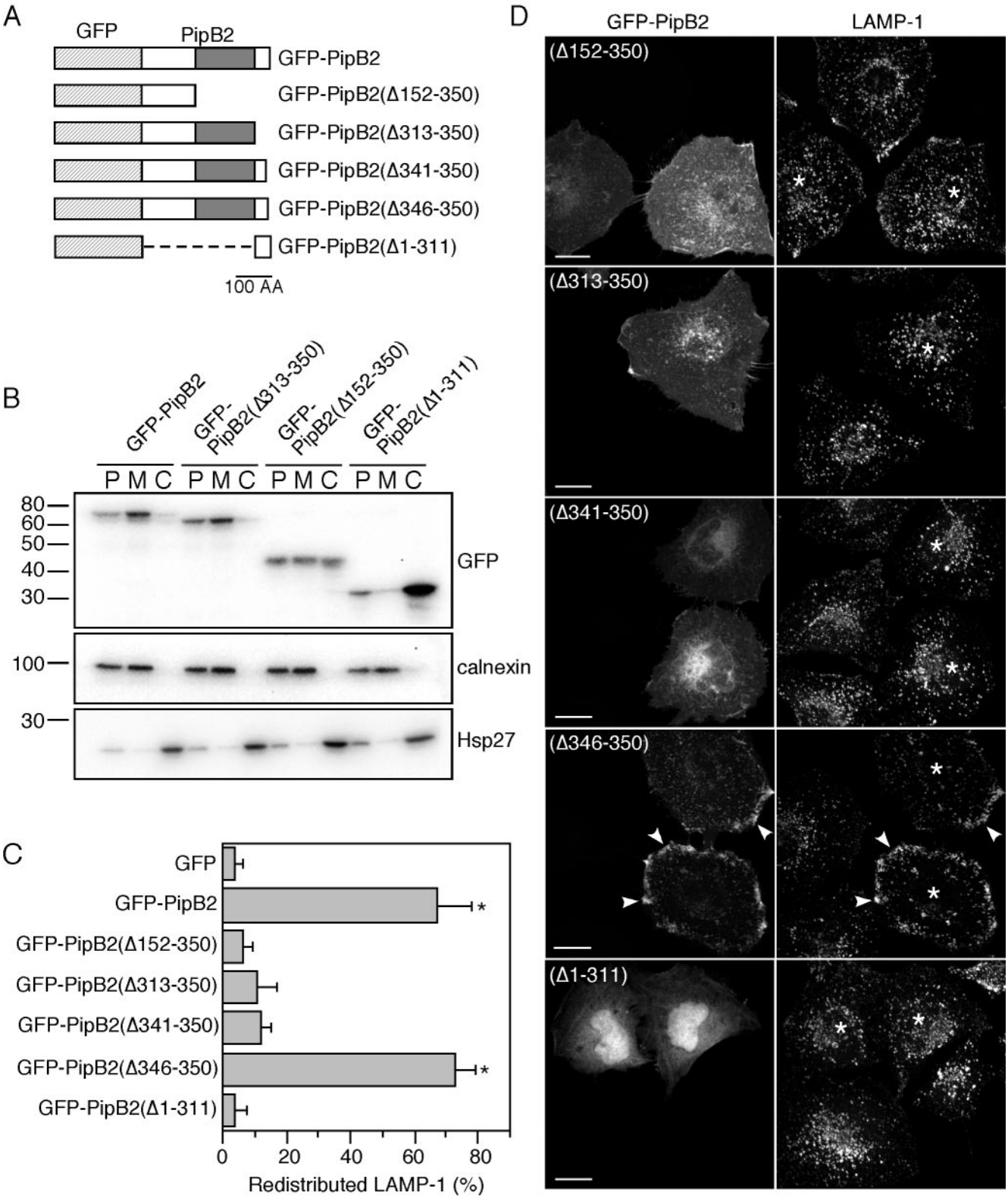

Figure 6. Domain analysis of PipB2. (A) Schematic of pGFP-PipB2 constructs. Hatched box represents GFP; gray box represents the pentapeptide-repeat region of PipB2. Bar, 100 amino acid residues. (B) GFP-PipB2 is associated with cell membranes. HeLa cells were transiently transfected for 24 h with the indicated constructs. Cells were mechanically disrupted and separated by differential centrifugation into three fractions: nuclei, cytoskeleton, and unbroken cells (P); membranes (M); and cytosol (C). Fractions were subject to immunoblot analysis for GFP-PipB2 fusion; an integral membrane protein, calnexin; or the cytosolic protein, Hsp27. Molecular mass markers are indicated on the left (in kilodaltons). (C) Quantification of LAMP-1 redistribution in HeLa cells after 24 h transfection with the indicated plasmids. Monolayers were fixed, permeabilized, and immunostained for LAMP-1. At least 100 transfected cells were scored by fluorescence

fused to GFP [pGFP-PipB2(Δ1-311)] localized to the nucleus and cytoplasm (Figure 6D), in agreement with the subcellular fractionation data (Figure 6B), and it did not alter LE/Lys positioning (Figure 6C). Collectively, these results indicate that both membrane association and amino acid residues 341–345 are required for the peripheral accumulation of PipB2 and LE/Lys.

A Pentapeptide Motif of PipB2 Is Essential for Peripheral Targeting and Redistribution of LE/Lys

To absolutely define the role of residues 341–345, we made an internal deletion of these residues (LFNEF; Figure 7B) and examined the effect on localization of GFP-PipB2 and LE/Lys 24 h after transfection. Figure 7A shows that GFP-PipB2(Δ341-345) neither accumulated at the cell periphery nor affected LE/Lys positioning. To address whether the LFNEF motif also was essential when PipB2 was bacterially delivered, Δ*pipB2* bacteria were complemented in trans with the corresponding deletion mutant [p*pipB2(Δ341-345)-2HA*]. HeLa cells were infected for 12 h and immunostained with α-HA to detect translocated PipB2(Δ341-345)-2HA, α-LPS, and α-LAMP-2. No peripheral accumulation of PipB2(Δ341-345)-2HA or LE/Lys was observed (Figure 7A). Furthermore, in contrast to full-length PipB2-2HA, in trans complementation with PipB2 lacking these five residues did not reduce Sif frequency compared with Δ*pipB2* or wild-type infections (Table 2). These data unequivocally demonstrate that residues 341–345 of PipB2 are essential for its intracellular targeting and biological actions on LE/Lys.

To identify which amino acid(s) in the LFNEF motif is(are) responsible for these activities, we made single point mutations substituting alanine for each residue. Transfected HeLa cells were subsequently scored for peripheral GFP-PipB2 and redistributed LE/Lys (Figure 7C). Mutation of each residue within the LFNEF motif had an effect GFP-PipB2 or LE/Lys localization, albeit with different phenotypes, whereas mutation of residues adjacent to the LFNEF motif, T340A and Y346F, had no effect (Figure 7C; our unpublished data). Surprisingly, an L341A mutation prevented the peripheral accumulation of GFP-PipB2 but only modestly affected its LE/Lys redistribution properties. This demonstrates that a peripheral concentration of GFP-PipB2 is not essential for the redistribution of LE/Lys. Conversely, an F345A substitution did not affect the peripheral accumulation of GFP-PipB2 but completely prevented LE/Lys redistribution. The F342A mutation resulted in an intermediate phenotype; a partial reduction in the peripheral accumulation of GFP-PipB2 and LAMP-1. Finally, the N343A and E344A substitutions had no effect on the peripheral accumulation of GFP-PipB2 but opposite effects on LE/Lys, increasing and decreasing LAMP-1 redistribution, respectively. In summary, mutation of each residue in the LFNEF motif affected the biological activity of GFP-PipB2 but not necessarily its localization. Therefore, no single residue in the LFNEF motif is required for both the peripheral targeting of PipB2 and repositioning of LE/Lys compartments. Rather the entire pentapeptide motif dictates these properties.

Figure 6 (cont). microscopy for peripheral LAMP-1 per experiment. Results are the mean ± SD from three separate experiments. Data points significantly different from GFP only transfection are indicated by asterisks ($p < 0.001$) (D) Representative confocal images from transfections. Asterisks indicate transfected cells and arrowheads indicate peripheral accumulation of GFP-PipB2(Δ346-350) and LAMP-1. Bar, 20 μm.

DISCUSSION

Although Sifs were first described over a decade ago (Garcia-del Portillo *et al*., 1993), how and why they are formed remains a mystery. Regardless, it is apparent that *Salmonella*-induced tubulation of LE/Lys compartments is essential for an optimal infection (Stein *et al*., 1996; Beuzon *et al*., 2000; Kuhle and Hensel, 2002; Boucrot *et al*., 2003). Previously, we identified two *Salmonella* type III effector homologues, PipB and PipB2, which are translocated by the SPI2 TTSS and localize to the SCV and Sifs (Knodler *et al*., 2002, 2003). Here, we demonstrate that the biological activity of PipB2 is required for the reorganization of LE/Lys during a *Salmonella* infection. When translocated by *Salmonella*, this activity results in the centrifugal extension of lgp-rich Sif tubules away from the SCV. On overexpression of *pipB2*, its biological activity is amplified, causing LE/Lys to accumulate at the cell periphery. PipB2 is the first bacterial effector identified with this property; however, other *Salmonella* type III effectors also must contribute to Sif elongation because a Δ*pipB2* mutant can initiate and partially extend Sifs away from the perinuclear SCV. The PipB2 homologue PipB does not seem to be required for this phenomenon. Possible candidates include SifA, SseF, SseG, or SopD2, mutants of which are defective for different aspects of Sif formation (Stein *et al*., 1996; Guy *et al*., 2000; Kuhle and Hensel, 2002; Jiang *et al*., 2004) or other, as yet undiscovered, *Salmonella* effectors. Ectopic expression of a subset of these SPI-2 TTSS effectors in mammalian cells affects the organization of LE/Lys, revealing their ability to manipulate this compartment. For example, ectopic expression of SifA, SpiC and SopD2 in mammalian cells leads to an increased perinuclear aggregation of LE/Lys (Brumell *et al*., 2001; Boucrot *et al*., 2003; Brumell *et al*., 2003; Shotland *et al*., 2003). Here, we have shown that, in contrast to these *Salmonella* effectors, ectopic expression of PipB2 induces the dispersal of LE/Lys toward the cell periphery. This suggests that opposing, as well as complementary, activities of multiple *Salmonella* effectors are required for Sif formation and homeostasis in host cells.

Type III translocated PipB2 localizes to SCV and Sifs and shows considerable overlap with LE/Lys markers (Figure 2A). Yet, upon overexpression, PipB2 targets peripheral tubular-vesicular structures that only partially colocalize with redistributed LAMPs (Figures 2–5). The identity of the PipB2$^+$, LAMP$^-$ compartment is currently unknown; it may represent a LAMP$^-$ subcompartment of LE/Lys or a non-LE/Lys compartment. Notably, NDZ treatment induces extensive colocalization between PipB2 and LE/Lys markers (Figure 5A), similar to what has been described for Rab7 and lysosomes (Méresse *et al*., 1995). This demonstrates that the PipB2$^+$, LAMP$^-$ compartments interconnect with LAMP$^+$ compartments (LE/Lys) by transport along microtubules.

We have shown that PipB2 acts specifically to redistribute LE/Lys and not other cellular organelles, although the mechanism by which this occurs remains to be established. In mammalian cells, LE/Lys can move bidirectionally but occupy a predominantly perinuclear location at steady state with their net direction of movement toward the MTOC. Their centripetal/retrograde movement is primarily mediated by Rab7, RILP, and dynein/dynactin (Valetti *et al*., 1999; Bucci *et al*., 2000; Cantalupo *et al*., 2001; Jordens *et al*., 2001), and their centrifugal/anterograde movement requires

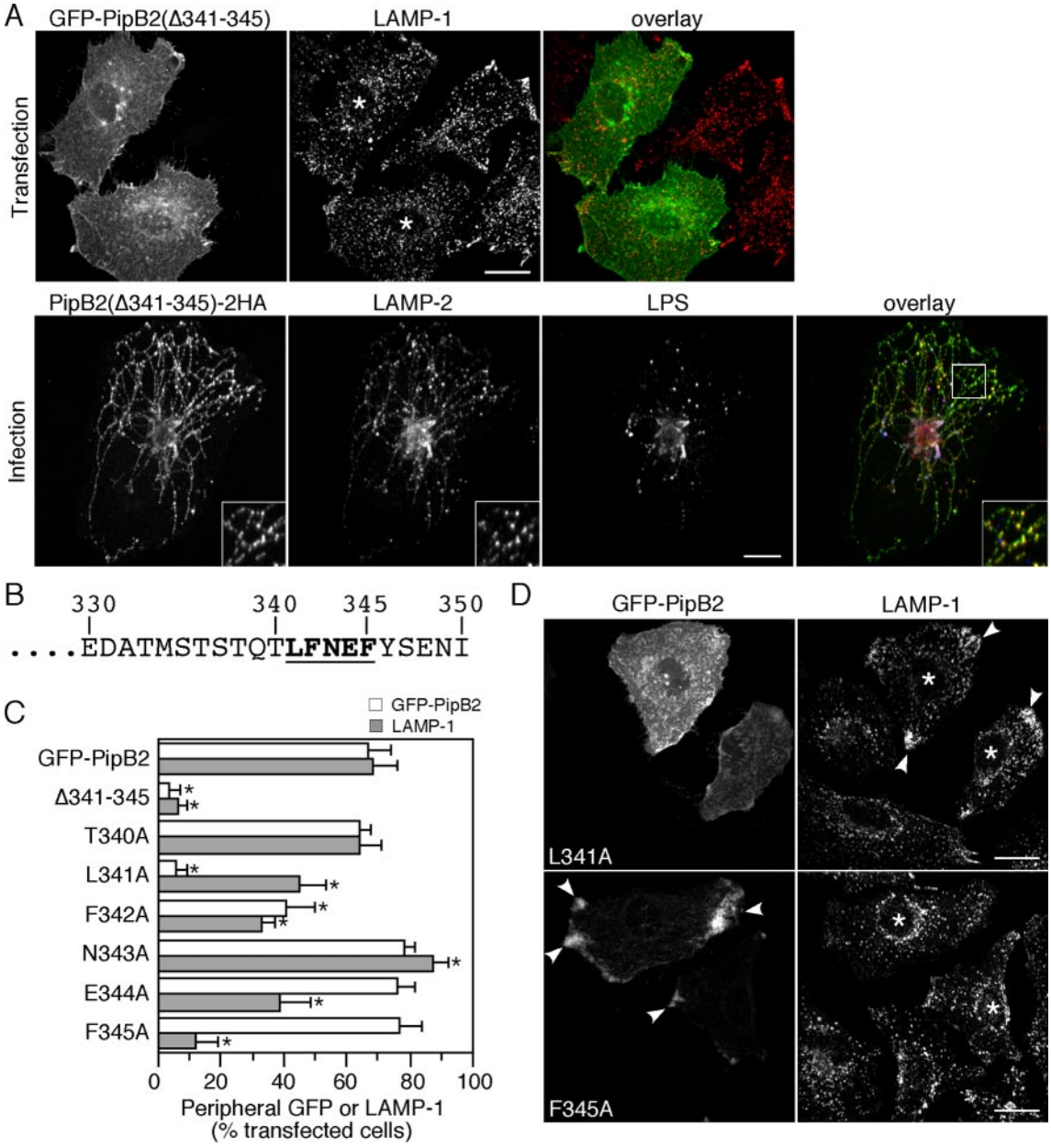

Figure 7. Residues 341–345 of PipB2 are required for peripheral targeting and relocation of LE/Lys. (A) Confocal micrographs showing localization of GFP-PipB2(Δ341-345) after transfection (top) and PipB2(Δ341-345)-2HA after bacterial translocation (bottom). Top, HeLa cells were transfected for 24 h with pGFP-PipB2(Δ341-345), fixed, permeabilized, and immunostained for LAMP-1. An overlay of the two images is shown on the right (GFP-PipB2(Δ341-345), green; and LAMP-1, red). Asterisks indicate transfected cells. Bar, 20 μm. Bottom, HeLa cells were infected with Δ*pipB2* p*pipB2(Δ341-345)-2HA* bacteria and processed for immunofluorescence at 12 h p.i. to detect PipB2(Δ341-345)-2HA (shown as green in overlay), LAMP-2 (red), and *Salmonella* LPS (blue). An overlay of the three images is presented on the right. Inset shows 2× enlargement of the boxed area. Bar, 10 μm. (B) Primary amino acid sequence of the PipB2 C terminus. Numbers denote specific residues in the PipB2 sequence. In bold and underlined is the region subject to mutational analysis. (C) Peripheral GFP localization and LAMP-1 redistribution for the various pGFP-PipB2 point mutants. HeLa cells were transfected for 24 h with the indicated mutants and then processed for immunofluorescence against LAMP-1. For each experiment, at least 100 transfected cells were scored by fluorescence microscopy for peripheral GFP-PipB2 (white bars) or LAMP-1 (gray bars). Results are the mean ± SD from three separate experiments. Data points significantly different from GFP-PipB2 transfection are marked by asterisks ($p < 0.001$). (D) Representative confocal images from transfections. Asterisks indicate transfected cells and arrowheads indicate peripheral LAMP-1 (top) and GFP-PipB2 F345A (bottom). Bar, 20 μm.

numerous microtubule plus end kinesin motors (Nakata and Hirokawa, 1995; Yamazaki *et al*., 1995; Santama *et al*., 1998; Bananis *et al*., 2004; Matsushita *et al*., 2004). These same proteins also are implicated in *Salmonella*-induced LE/Lys aggregation and tubulation (Brumell *et al*., 2001; Guignot *et al*., 2004; Harrison *et al*., 2004) and maintenance of the SCV membrane (Boucrot *et al*., 2005). Our results suggest that PipB2 increases the net anterograde movement of LE/Lys. Possible mechanisms include modulation of the binding of motor protein receptors or motor proteins themselves to LE/Lys, the activity of motor proteins, or increased microtubule polymerization. Another *Salmonella* effector, SifA, has

recently been shown to regulate SCV membrane dynamics by down-regulating kinesin activity associated with the SCV via its interaction with SKIP (Boucrot *et al*., 2005). SifA also is proposed to affect motor recruitment to Sifs; SifA binding to Rab7 displaces RILP/dynein-dynactin from Sifs, resulting in their centrifugal extension (Harrison *et al*., 2004). We have no evidence that PipB2 binds Rab7 (our unpublished data), and our cotransfection studies suggest that PipB2 acts downstream or in a parallel pathway to this small GTPase. Thus, it is unlikely that PipB2 and SifA contribute to Sif formation in the same manner.

Our studies demonstrate that at least two regions of PipB2 act as targeting determinants in mammalian cells. First, PipB2 stably associates with tubular-vesicular membranes via its N-terminal domain. This could be a direct association or indirect by binding to a mammalian membrane-associated protein. We have further identified an LFNEF motif in the C terminus of PipB2 (residues 341–345) that is essential for its peripheral localization and effects on LE/Lys positioning. Notably, both membrane association and the LFNEF motif are requisite for PipB2 peripheral targeting and biological activity. The homologue PipB also is membrane associated (Knodler *et al*., 2003), but it does not possess this LFNEF motif or biological functions similar to PipB2. However, addition of the LFNEF motif to PipB does not confer PipB2-like biological activity. Therefore, sequence motifs in addition to LFENF are required for the biochemical functions of PipB2. An interesting observation is that the LFNEF motif is very similar to peptide motifs found in mammalian "accessory proteins" that are involved in vesicular membrane trafficking. Via this motif, accessory proteins such as Rabaptin 5, γ-synergin, and EpsinR/Clint/Enthoprotin bind to vesicle-associated adaptor proteins including adaptor protein-1 (AP-1) and Golgi-localized, γ ear-containing Arf binding proteins (GGAs) (Mattera *et al*., 2004; Ritter *et al*., 2004). The function of these low-affinity protein–protein interactions is currently unknown, although modulation of vesicle targeting, fusion or cargo selection has been suggested (Bonifacino, 2004). We found that ectopic expression of GFP-PipB2 induces the peripheral accumulation of a subset of AP-1, GGA3, and clathrin-positive structures (our unpublished data), but we were unable to detect a direct interaction between PipB2 and adaptor proteins by yeast two-hybrid, coimmunoprecipitation, or pull downs. Therefore, it remains unresolved whether PipB2 binds to vesicle adaptors via its LFNEF motif to affect LE/Lys positioning.

Analogous to *Salmonella* invasion of mammalian cells, it is now apparent that the concerted actions of many type III effectors are required for establishment of its vacuolar niche. To date, seven *Salmonella* proteins have been shown to regulate Sif tubule biogenesis—SifA (Stein *et al*., 1996), SseF, SseG (Guy *et al*., 2000; Kuhle and Hensel, 2002), SopD2 (Jiang *et al*., 2004), SseJ, SpvB (Birmingham *et al*., 2005), and PipB2 (this study). But many questions remain unanswered. What are their mechanisms of action? How are their actions coordinated? Are these effectors translocated simultaneously or temporally? One major reason for this is that most effector deletion mutants have little or no phenotype in vitro or in vivo. In this respect, what we describe here for PipB2 is unique—a detectable phenotype in tissue culture cells whether *pipB2* is deleted, overexpressed from bacteria or ectopically expressed. This provides us with a useful tool to investigate how *Salmonella* uses PipB2 to modulate the host cell's endosomal system and create the intracellular niche that is so important for successful colonization and pathogenesis. Unraveling these details will not only yield important information about host–pathogen interactions but also help us to answer fundamental cell biological questions concerning endosomal movement and organelle positioning in mammalian cells.

ACKNOWLEDGMENTS

We thank Rey Carabeo, Jean Celli, Dan Drecktrah, Scott Grieshaber, Dale Howe, and Stéphane Méresse for critical reading of this manuscript. We are grateful to Cecilia Bucci, Wanjin Hong, Jean Gruenberg, Minoru Fukuda, Walter Gregory, and Stuart Kornfeld for plasmids and antibodies. We also thank Rafael Mattera, Juan Bonifacino, and Linton Traub for helpful discussions and the Murdock DNA Sequencing Facility at the University of Montana and the Genomics Core Facility at Rocky Mountain Labs for DNA sequencing analysis.

REFERENCES

Bananis, E., Nath, S., Gordon, K., Satir, P., Stockert, R. J., Murray, J. W., and Wolkoff, A. W. (2004). Microtubule-dependent movement of late endocytic vesicles *in vitro*: requirements for Dynein and Kinesin. Mol. Biol. Cell *15*, 3688–3697.

Bateman, A., Murzin, A. G., and Teichmann, S. A. (1998). Structure and distribution of pentapeptide repeats in bacteria. Protein Sci. *7*, 1477–1480.

Beuzon, C. R., Méresse, S., Unsworth, K. E., Ruiz-Albert, J., Garvis, S., Waterman, S. R., Ryder, T. A., Boucrot, E., and Holden, D. W. (2000). *Salmonella* maintains the integrity of its intracellular vacuole through the action of SifA. EMBO J. *19*, 3235–3249.

Birmingham, C. L., Jiang, X., Ohlson, M. B., Miller, S. I., and Brumell, J. H. (2005). *Salmonella*-induced filament formation is a dynamic phenotype induced by rapidly replicating *Salmonella enterica* serovar *typhimurium* in epithelial cells. Infect. Immun. *73*, 1204–1208.

Bonifacino, J. S. (2004). The GGA proteins: adaptors on the move. Nat. Rev. Mol. Cell. Biol. *5*, 23–32.

Boucrot, E., Beuzon, C. R., Holden, D. W., Gorvel, J. P., and Méresse, S. (2003). Salmonella typhimurium SifA effector protein requires its membrane-anchoring C-terminal hexapeptide for its biological function. J. Biol. Chem. *278*, 14196–14202.

Boucrot, E., Henry, T., Borg, J. P., Gorvel, J. P., and Méresse, S. (2005). The intracellular fate of *Salmonella* depends on the recruitment of kinesin. Science *308*, 1174–1178.

Brumell, J. H., Goosney, D. L., and Finlay, B. B. (2002). SifA, a type III secreted effector of *Salmonella typhimurium*, directs *Salmonella*-induced filament (Sif) formation along microtubules. Traffic *3*, 407–415.

Brumell, J. H., Kujat-Choy, S., Brown, N. F., Vallance, B. A., Knodler, L. A., and Finlay, B. B. (2003). SopD2 is a novel type III secreted effector of *Salmonella typhimurium* that targets late endocytic compartments upon delivery into host cells. Traffic *4*, 36–48.

Brumell, J. H., Tang, P., Mills, S. D., and Finlay, B. B. (2001). Characterization of *Salmonella*-induced filaments (Sifs) reveals a delayed interaction between *Salmonella*-containing vacuoles and late endocytic compartments. Traffic *2*, 643–653.

Bucci, C., Thomsen, P., Nicoziani, P., McCarthy, J., and van Deurs, B. (2000). Rab *7*, a key to lysosome biogenesis. Mol. Biol. Cell *11*, 467–480.

Burkhardt, J. K., Echeverri, C. J., Nilsson, T., and Vallee, R. B. (1997). Overexpression of the dynamitin (p50) subunit of the dynactin complex disrupts dynein-dependent maintenance of membrane organelle distribution. J. Cell Biol. *139*, 469–484.

Cain, R. J., Hayward, R. D., and Koronakis, V. (2004). The target cell plasma membrane is a critical interface for *Salmonella* cell entry effector-host interplay. Mol. Microbiol. *54*, 887–904.

Cantalupo, G., Alifano, P., Roberti, V., Bruni, C. B., and Bucci, C. (2001). Rab-interacting lysosomal protein (RILP): the Rab7 effector required for transport to lysosomes. EMBO J. *20*, 683–693.

Caplan, S., Hartnell, L. M., Aguilar, R. C., Naslavsky, N., and Bonifacino, J. S. (2001). Human Vam6p promotes lysosome clustering and fusion *in vivo*. J. Cell Biol. *154*, 109–122.

Carlsson, S. R., Roth, J., Piller, F., and Fukuda, M. (1988). Isolation and characterization of human lysosomal membrane glycoproteins, h-lamp-1 and h-lamp-2. Major sialoglycoproteins carrying polylactosaminoglycan. J. Biol. Chem. *263*, 18911–18919.

Cirillo, D. M., Valdivia, R. H., Monack, D. M., and Falkow, S. (1998). Macrophage-dependent induction of the *Salmonella* pathogenicity island 2 type III

secretion system and its role in intracellular survival. Mol. Microbiol. *30*, 175–188.

Drecktrah, D., Knodler, L. A., Galbraith, K., and Steele-Mortimer, O. (2005). The *Salmonella* SPI1 effector SopB stimulates nitric oxide production long after invasion. Cell. Microbiol. *7*, 105–113.

Freeman, J. A., Ohl, M. E., and Miller, S. I. (2003). The *Salmonella enterica* serovar typhimurium translocated effectors SseJ and SifB are targeted to the *Salmonella*-containing vacuole. Infect. Immun. *71*, 418–427.

Garcia-del Portillo, F., and Finlay, B. B. (1995). Targeting of *Salmonella typhimurium* to vesicles containing lysosomal membrane glycoproteins bypasses compartments with mannose 6-phosphate receptors. J. Cell Biol. *129*, 81–97.

Garcia-del Portillo, F., Zwick, M. B., Leung, K. Y., and Finlay, B. B. (1993). *Salmonella* induces the formation of filamentous structures containing lysosomal membrane glycoproteins in epithelial cells. Proc. Natl. Acad. Sci. USA *90*, 10544–10548.

Guignot, J., Caron, E., Beuzon, C., Bucci, C., Kagan, J., Roy, C., and Holden, D. W. (2004). Microtubule motors control membrane dynamics of *Salmonella*-containing vacuoles. J. Cell Sci. *117*, 1033–1045.

Guy, R. L., Gonias, L. A., and Stein, M. A. (2000). Aggregation of host endosomes by *Salmonella* requires SPI2 translocation of SseFG and involves SpvR and the fms-aroE intragenic region. Mol. Microbiol. *37*, 1417–1435.

Harrison, R. E., Brumell, J. H., Khandani, A., Bucci, C., Scott, C. C., Jiang, X., Finlay, B. B., and Grinstein, S. (2004). *Salmonella* impairs RILP recruitment to Rab7 during maturation of invasion vacuoles. Mol. Biol. Cell *15*, 3146–3154.

Hensel, M. (2004). Evolution of pathogenicity islands of *Salmonella enterica*. Int. J. Med. Microbiol. *294*, 95–102.

Hensel, M., Shea, J. E., Waterman, S. R., Mundy, R., Nikolaus, T., Banks, G., Vazquez-Torres, A., Gleeson, C., Fang, F. C., and Holden, D. W. (1998). Genes encoding putative effector proteins of the type III secretion system of *Salmonella* pathogenicity island 2 are required for bacterial virulence and proliferation in macrophages. Mol. Microbiol. *30*, 163–174.

Hernandez, L. D., Hueffer, K., Wenk, M. R., and Galan, J. E. (2004). *Salmonella* modulates vesicular traffic by altering phosphoinositide metabolism. Science *304*, 1805–1807.

Hollenbeck, P. J., and Swanson, J. A. (1990). Radial extension of macrophage tubular lysosomes supported by kinesin. Nature *346*, 864–866.

Horton, R. M., Hunt, H. D., Ho, S. N., Pullen, J. K., and Pease, L. R. (1989). Engineering hybrid genes without the use of restriction enzymes: gene splicing by overlap extension. Gene *77*, 61–68.

Jiang, X., Rossanese, O. W., Brown, N. F., Kujat-Choy, S., Galan, J. E., Finlay, B. B., and Brumell, J. H. (2004). The related effector proteins SopD and SopD2 from *Salmonella enterica* serovar Typhimurium contribute to virulence during systemic infection of mice. Mol. Microbiol. *54*, 1186–1198.

Jordens, I., Fernandez-Borja, M., Marsman, M., Dusseljee, S., Janssen, L., Calafat, J., Janssen, H., Wubbolts, R., and Neefjes, J. (2001). The Rab7 effector protein RILP controls lysosomal transport by inducing the recruitment of dynein-dynactin motors. Curr. Biol. *11*, 1680–1685.

Knodler, L. A., Celli, J., Hardt, W. D., Vallance, B. A., Yip, C., and Finlay, B. B. (2002). *Salmonella* effectors within a single pathogenicity island are differentially expressed and translocated by separate type III secretion systems. Mol. Microbiol. *43*, 1089–1103.

Knodler, L. A., and Steele-Mortimer, O. (2003). Taking possession: biogenesis of the *Salmonella*-containing vacuole. Traffic *4*, 587–599.

Knodler, L. A., Vallance, B. A., Hensel, M., Jackel, D., Finlay, B. B., and Steele-Mortimer, O. (2003). *Salmonella* type III effectors PipB and PipB2 are targeted to detergent-resistant microdomains on internal host cell membranes. Mol. Microbiol. *49*, 685–704.

Kuhle, V., and Hensel, M. (2002). SseF and SseG are translocated effectors of the type III secretion system of *Salmonella* pathogenicity island 2 that modulate aggregation of endosomal compartments. Cell. Microbiol. *4*, 813–824.

Kuhle, V., and Hensel, M. (2004). Cellular microbiology of intracellular *Salmonella enterica*: functions of the type III secretion system encoded by *Salmonella* pathogenicity island 2. Cell. Mol. Life Sci. *61*, 2812–2826.

Lane, J., and Allan, V. (1998). Microtubule-based membrane movement. Biochim. Biophys. Acta *1376*, 27–55.

Mallik, R., and Gross, S. P. (2004). Molecular motors: strategies to get along. Curr. Biol. *14*, R971–982.

Marsman, M., Jordens, I., Kuijl, C., Janssen, L., and Neefjes, J. (2004). Dynein-mediated vesicle transport controls intracellular *Salmonella* replication. Mol. Biol. Cell *15*, 2954–2964.

Matsushita, M., Tanaka, S., Nakamura, N., Inoue, H., and Kanazawa, H. (2004). A novel kinesin-like protein, KIF1Bbeta3 is involved in the movement of lysosomes to the cell periphery in non-neuronal cells. Traffic *5*, 140–151.

Mattera, R., Ritter, B., Sidhu, S. S., McPherson, P. S., and Bonifacino, J. S. (2004). Definition of the consensus motif recognized by γ-adaptin ear domains. J. Biol. Chem. *279*, 8018–8028.

Méresse, S., Gorvel, J. P., and Chavrier, P. (1995). The rab7 GTPase resides on a vesicular compartment connected to lysosomes. J. Cell Sci. *108*, 3349–3358.

Méresse, S., Steele-Mortimer, O., Finlay, B. B., and Gorvel, J. P. (1999). The rab7 GTPase controls the maturation of *Salmonella* typhimurium-containing vacuoles in HeLa cells. EMBO J. *18*, 4394–4403.

Mizuno, K., Kitamura, A., and Sasaki, T. (2003). Rabring7, a novel Rab7 target protein with a RING finger motif. Mol. Biol. Cell *14*, 3741–3752.

Morgan, E., Campbell, J. D., Rowe, S. C., Bispham, J., Stevens, M. P., Bowen, A. J., Barrow, P. A., Maskell, D. J., and Wallis, T. S. (2004). Identification of host-specific colonization factors of *Salmonella enterica* serovar *typhimurium*. Mol. Microbiol. *54*, 994–1010.

Nakata, T., and Hirokawa, N. (1995). Point mutation of adenosine triphosphate-binding motif generated rigor kinesin that selectively blocks anterograde lysosome membrane transport. J. Cell Biol. *131*, 1039–1053.

Patel, J. C., and Galan, J. E. (2005). Manipulation of the host actin cytoskeleton by *Salmonella* - all in the name of entry. Curr. Opin. Microbiol. *8*, 10–15.

Poupon, V., Stewart, A., Gray, S. R., Piper, R. C., and Luzio, J. P. (2003). The role of mVps18p in clustering, fusion, and intracellular localization of late endocytic organelles. Mol. Biol. Cell *14*, 4015–4027.

Press, B., Feng, Y., Hoflack, B., and Wandinger-Ness, A. (1998). Mutant Rab7 causes the accumulation of cathepsin D and cation-independent mannose 6-phosphate receptor in an early endocytic compartment. J. Cell Biol. *140*, 1075–1089.

Ritter, B., Denisov, A. Y., Philie, J., Deprez, C., Tung, E. C., Gehring, K., and McPherson, P. S. (2004). Two WXXF-based motifs in NECAPs define the specificity of accessory protein binding to AP-1 and AP-2. EMBO J. *23*, 3701–3710.

Ruiz-Albert, J., Yu, X. J., Beuzon, C. R., Blakey, A. N., Galyov, E. E., and Holden, D. W. (2002). Complementary activities of SseJ and SifA regulate dynamics of the *Salmonella typhimurium* vacuolar membrane. Mol. Microbiol. *44*, 645–661.

Salcedo, S. P., and Holden, D. W. (2003). SseG, a virulence protein that targets *Salmonella* to the Golgi network. EMBO J. *22*, 5003–5014.

Santama, N., Krijnse-Locker, J., Griffiths, G., Noda, Y., Hirokawa, N., and Dotti, C. G. (1998). KIF2β, a new kinesin superfamily protein in non-neuronal cells, is associated with lysosomes and may be implicated in their centrifugal translocation. EMBO J. *17*, 5855–5867.

Scott, C. C., Cuellar-Mata, P., Matsuo, T., Davidson, H. W., and Grinstein, S. (2002). Role of 3-phosphoinositides in the maturation of *Salmonella*-containing vacuoles within host cells. J. Biol. Chem. *277*, 12770–12776.

Shotland, Y., Kramer, H., and Groisman, E. A. (2003). The *Salmonella* SpiC protein targets the mammalian Hook3 protein function to alter cellular trafficking. Mol. Microbiol. *49*, 1565–1576.

Steele-Mortimer, O., Méresse, S., Gorvel, J. P., Toh, B. H., and Finlay, B. B. (1999). Biogenesis of *Salmonella typhimurium*-containing vacuoles in epithelial cells involves interactions with the early endocytic pathway. Cell Microbiol. *1*, 33–49.

Stein, M. A., Leung, K. Y., Zwick, M., Garcia-del Portillo, F., and Finlay, B. B. (1996). Identification of a *Salmonella* virulence gene required for formation of filamentous structures containing lysosomal membrane glycoproteins within epithelial cells. Mol. Microbiol. *20*, 151–164.

Valdivia, R. H., and Falkow, S. (1997). Fluorescence-based isolation of bacterial genes expressed within host cells. Science *277*, 2007–2011.

Valetti, C., Wetzel, D. M., Schrader, M., Hasbani, M. J., Gill, S. R., Kreis, T. E., and Schroer, T. A. (1999). Role of dynactin in endocytic traffic: effects of dynamitin overexpression and colocalization with CLIP-170. Mol. Biol. Cell *10*, 4107–4120.

Wang, T., and Hong, W. (2002). Interorganellar regulation of lysosome positioning by the Golgi apparatus through Rab34 interaction with Rab-interacting lysosomal protein. Mol. Biol. Cell *13*, 4317–4332.

Wang, T., Wong, K. K., and Hong, W. (2004). A unique region of RILP distinguishes it from its related proteins in its regulation of lysosomal morphology and interaction with Rab7 and Rab34. Mol. Biol. Cell *15*, 815–826.

Waterman, S. R., and Holden, D. W. (2003). Functions and effectors of the *Salmonella* pathogenicity island 2 type III secretion system. Cell Microbiol. *5*, 501–511.

Wood, M. W., Jones, M. A., Watson, P. R., Hedges, S., Wallis, T. S., and Galyov, E. E. (1998). Identification of a pathogenicity island required for *Salmonella* enteropathogenicity. Mol. Microbiol. *29*, 883–891.

Yamazaki, H., Nakata, T., Okada, Y., and Hirokawa, N. (1995). KIF3A/B: a heterodimeric kinesin superfamily protein that works as a microtubule plus end-directed motor for membrane organelle transport. J. Cell Biol. *130*, 1387–1399.